PROMOTING TRANSIT

IN THE MULTIMODAL TRAFFIC ENVIRONMENT

LIYU WU

PhD

The Hong Kong Polytechnic University

2021

The Hong Kong Polytechnic University

Department of Electrical Engineering

Promoting Transit in the Multimodal Traffic Environment

Liyu Wu

A thesis submitted in partial fulfillment of the

requirements for the degree of

Doctor of Philosophy

August 2020

CERTIFICATE OF ORIGINALITY

I hereby declare that this thesis is my own work and that, to the best of my knowledge and belief, it reproduces no material previously published or written, nor material that has been accepted for the award of any other degree or diploma, except where due acknowledgement has been made in the text.

_____ (Signed)

_____Liyu Wu_____(Name of student)

Abstract

Public transit is an effective method for combating traffic congestion in large cities where transit vehicles co-exist with other traffic modes such as cars and bicycles. However, present designs and operations of transit systems seldom consider the multimodal feature of urban traffic environment. In light of this, the present thesis explores optimal designs and efficient strategies for promoting transit systems. The study covers both the macroscopic (city-wide) and microscopic (city-block) scales.

At the city-wide scale, we consider the design of an idealized transit network that can be accessed via shared bikes, since those bikes have become increasingly popular in many cities. Patrons may walk to shared-bike docking stations nearest their origins, and then cycle to their nearest transit stations where they deposit the bikes. The travel pattern is reversed when patrons cycle from their final transit stations on to their destinations. Patrons choose between this option and that of solely walking to or from transit stations. Shared bikes are priced to achieve the system-optimal assignment of the two feeder options.

The idealized transit network is laid-out in hybrid fashion, where transit lines form square grids inside city centers, and radiate outward in the peripheries. A set of simplifying assumptions are adopted that pertain primarily to the nature of travel demand. These enable the formulation of a parsimonious, continuous model. The model produces designs that minimize total travel costs, and is ideally suited for high-level (i.e., strategic) planning. Similar models are developed for systems in which access or egress to or from transit can occur solely by walking, and by walking and riding fixed-route feeder buses in combination.

Comparisons of these feeder options are drawn through numerical analyses. These are performed in parametric fashion by varying city size, travel demand, and economic conditions; and for trunk services that are provided either by ordinary buses, Bus Rapid Transit, or metro rail. Designs are produced for cases in which shared-bike and feeder-bus services are made to fit pre-existing and unchangeable trunk-line networks; and for cases in which trunk and feeder services are optimized jointly. Outcomes reveal that shared-bike feeder systems can virtually always reduce costs over walking alone, with cost savings as high as 7%, even when the shared bikes are made to fit a pre-existing transit network. Shared-biking often outperforms feeder-bus service as well. We further find that the joint optimization of trunk and shared-bike feeder

services can reduce costs not only to users, but also to the transit agency that operates these services. Savings to the agency can be used to subsidize shared-bike services. We show that with or without this subsidy, shared-bike systems can always break even when they are suitably priced, and jointly optimized with trunk service.

At the city-block scale, we consider a typical busy intersection approach controlled by a traffic signal, where buses and cars compete for green time and lane space. Signalized intersections are common bottlenecks in urban transportation systems where cars and buses may suffer from long queues and large delays. Existing bus priority strategies often promote transit at the cost of reducing cars' discharging capacity and creating more delays for cars. To solve this dilemma, we use a mid-block pre-signal that sorts through-moving and left-turning cars to increase their discharge capacity, and that also allows buses to skip the car queues. The pre-signal is further integrated with transit signal priority (TSP) schemes to further reduce bus delays. We develop a dynamic TSP strategy that determines the optimal TSP scheme to implement given the real-time bus arrival information.

Analytical models are formulated to develop the car discharge capacity and the expected bus delay at the intersection approach. Trade-off between the above two metrics is examined. Numerical analysis is conducted for a wide range of operating settings with various bus arrival rates, numbers of lanes, and left-turning vehicle ratios. Our proposed intersection approach design with dynamic TSP strategy is compared against alternative designs. Results show that our design can greatly reduce bus delays without compromising cars' discharge capacity.

Acknowledgements

This thesis would not come into being if I had not received help from my supervisors, teammates, friends, and families. I would like to express my genuine gratitude to them, without who I could have already given up.

First of all, the profound gratitude must flow to my chief supervisor Dr. Weihua Gu, for his great patience and continuous support. He has walked me through the entire six years of my Ph. D study. His great perseverance in work, his constant pursuit of knowledge, and his meticulous attitude towards research manifest the personalities I should cultivate as a qualified researcher. I am indebted to him, not only for his invaluable instructions and insightful guidance, but also for his precious considerations and kindness. For many times I failed to proceed as planned, he gave me time and kept encouraging me to pursue my studies. I give my deepest gratitude to him for his generous help.

I would like to extend my sincere appreciation to my co-supervisor Dr. Ilgin Guler, for her encouragement, wisdom, kindness, and care in both my study and life. Many thanks also go to all the professors and senior researchers who have helped me a lot during my postgraduate study: Professor Wenbo Fan, Professor Alan Lau, Professor Edward Chung, Professor Xin Li, Professor Yiming Bie, Dr. Qiang Zeng, Dr. Jinwoo Lee. They always gave me valuable suggestions and illuminating comments, without which I would fumble many more years.

Also, I owe many thanks to my friends and teammates for all the companionship and good memories. To Samuel, Joy, Larry, Qiaolin, Xiao, Fangyi, Fuliang, and Ming: thank you for the days we worked together at Hong Kong, and for always being considerate and trying to cheer me up. To Zhengyao, Kan, and Lingyu: thank you for always taking good care of me and keeping me company during the endless blizzard at Penn State. In addition, a special thank you to my close friends: Hailey, Rayray, Xinyi, Siyu, Wenxi, and Lin, for the consistent friendship and support, wherever we are.

Finally, I would like to thank my beloved parents for their unfailing love and tremendous support. Thank you for bringing me to this wonderful world, and thank you for

always trusting and respecting me. I also feel so grateful to have Key, who brightened my life when I was in the valley of despair. Your love and company are the greatest fortune of my life.

Table of Contents

List of figures

Chapter 1

Introduction

Section 1.1 presents the background and motivation of this thesis. Section 1.2 furnishes an overview of the thesis.

1.1 Background and motivation

Public transit has been long recognized as a green and cost-effective means to combat the ever-growing travel demands and traffic congestion, especially in large metropolitan areas. Regrettably, most transit systems perform much worse than private cars, not only because of the first- and last-mile trip segments that are usually covered by walking only, but also due to the significant delays transit vehicles experience at stops and traffic signals.

In congested urban areas, transit vehicles, especially buses, are often operating in a multimodal urban environment consisting of cars, bicycles, etc. Thus, interactions between transit vehicles and other modes play a vital role in the operational efficiency of transit systems. Some of those interactions are cooperative and beneficial for the interacting modes, while others reflect competitions for limited resources (e.g., road space), and can be damaging to all interacting modes. To develop novel designs and operating strategies for improving urban transit performance (Watkins et al., 2019), these multimodal interactions must be accounted for. In light of the above, the present thesis will examine how transit performance can be improved under both types of interactions: cooperative interactions that can benefit transit by integrating other modes, and competing interactions with other modes that is potentially detrimental to transit.

Potential cooperation between transit and other modes is examined at the macroscopic, city-wide scale. Specifically, we focus on the integration of faster access/egress modes, e.g., shared bikes, with a transit network. As a sustainable and environmentally friendly model, shared bikes can conveniently solve the first- and last-mile problems of transit by enabling patrons to ride at one or both ends of their trips without carrying bicycles aboard transit vehicles (Liu et al., 2012). Moreover, the increased access and egress travel speed also makes longer transit stop spacings possible; and long stop spacings will in turn increase transit vehicles'

commercial speed, and reduce the transit agency's operating costs. Thus, the integration of shared bicycles and transit at the network level holds much promise to improve both the transit performance and the bike ridership.

On the other hand, buses traveling in mixed-traffic lanes need compete for the limited road space and traffic signal time with other vehicles (mostly cars). This competition is examined at the microscopic, city-block scale. Specifically, we consider how the signal time and lane space can be efficiently allocated at busy signalized intersections in a way that can improve performance of both bus and car traffic, as compared to the conventional, mixed-traffic operations. This is done by a novel design that integrates transit signal priority (TSP) with intermittent bus lane (IBLs) and mid-block pre-signals.

1.2 Overview of the thesis

The following two chapters explore the city-wide joint design of transit and bike-sharing networks, and the novel strategy for promoting both car and bus operations at signalized intersections.

Chapter 2 examines the optimal design of transit networks in which access and egress can occur via a shared-bike service. Patrons may walk to shared-bike docking stations nearest their origins, and then cycle to their nearest transit stations where they deposit the bikes. The travel pattern is reversed when patrons cycle from their final transit stations on to their destinations. Patrons choose between this option and that of solely walking to or from transit stations. We explore shared-bike pricing schemes to achieve the system-optimal assignment of the two feeder options.

We assume that transit trunk-line networks are laid-out in hybrid fashion, as proposed in Daganzo (2010a). Transit lines thus form square grids inside city centers, and radiate outward in the peripheries. As in Daganzo (2010a) and other studies, a set of simplifying assumptions are adopted that pertain primarily to the nature of travel demand. These enable the formulation of a parsimonious, continuous model. The model produces designs that minimize total travel costs, and is ideally suited for high-level (i.e., strategic) planning. A similar model is developed for systems in which access or egress to or from transit can occur solely by walking, or by walking and riding fixed-route feeder buses in combination. The shared-bike

and feeder-bus models both complement Daganzo's original model in which access and egress occur solely by walking.

Comparisons of these feeder options are drawn through numerical analyses. These are performed in parametric fashion by varying city size, travel demand, and economic conditions; and for trunk services that are provided either by ordinary buses, Bus Rapid Transit, or metro rail. Designs are produced for cases in which shared-bike and feeder-bus services are made to fit pre-existing and unchangeable trunk-line networks; and for cases in which trunk and feeder services are optimized jointly.

Our numerical results reveal that shared-bike feeder systems can often reduce costs over walking alone, with cost savings as high as 7%, even when the shared bikes are made to fit a pre-existing transit network. Shared-biking often outperforms feeder-bus service as well. We further find that the joint optimization of trunk and shared-bike feeder services can reduce costs not only to users, but also to the transit agency that operates these services. Savings to the agency can be used to subsidize shared-bike services. We show that with or without this subsidy, shared-bike systems can always break even when they are suitably priced, and jointly optimized with trunk service.

Chapter 3 models and tests a proposed design of signalized intersection approach that integrates a mid-block pre-signal, an intermittent bus lane, and various TSP schemes (i.e., green extension, red truncation, green insertion, and pre-signal green truncation) in a way that benefits both bus and car traffic. The strategy dynamically selects the best TSP scheme according to predicted bus arrival times in a target cycle. The pre-signal is multi-purpose in that it both prioritizes arriving buses and sorts out car traffic to increase their discharge capacity.

Analytical models are formulated to calculate two performance metrics: the expected car discharge capacity from the intersection approach and the expected bus delay. Trade-off between these two metrics is examined for the proposed design, and for a number of alternative scenarios for comparison. These include: (i) a "do-nothing" scenario that provides neither TSP nor bus lane, and uses no pre-signal; (ii) a pre-signal only scenario where a pre-signal is installed to sort car traffic as per Xuan et al. (2011), but no bus priority measure is provided; (iii) a scenario involving dedicated bus lane where buses enjoy TSP and a bus lane throughout the approach; and (iv) scenarios each involving a single-type TSP scheme instead of multiple TSP schemes selected dynamically and optimally.

Chapter 4 concludes the thesis by summarizing the contributions and discussing potential extensions of the thesis work.

Chapter 2

Optimal design of transit networks fed by shared bikes

2.1 Introduction and literature review

Public transit services can be accessed by feeder bus and, less commonly by bicycle. Both options are speedier than walking. Bicycles are less expensive than buses, however, and are more environmentally friendly (Pucher and Buehler, 2008, 2012). And for able-bodied travelers, bikes can be convenient to use, save perhaps in hilly cities and inclement weather. Little wonder that communities that deploy bike lanes and other bicycle-friendly facilities often find that ridership grows for transit as well as for bikes (Beatley, 2014; Bonnette, 2007; Hampshire and Marla, 2012; Martens, 2007; Noland and Ishaque, 2006; Wieth-Knudsen, 2012).

Shared bicycles that are rented by transit patrons seem a particularly promising means of feeder service (Goodyear, 2014; Gutman, 2017; Liu et al., 2012; Midgley, 2011; 2013; Shaheen et al., 2009, 2010; Wang, 2013a); and one that surveys suggest is preferred by many cyclists (TNS Sofres, 2009). Sharing relieves riders of having to purchase, maintain and protect their own bikes. And it conveniently solves transit's first- and last-mile problem by enabling patrons to ride at one or both ends of their trips without carrying bicycles aboard buses or trains (Liu et al., 2012). This is something that both transit patrons and operating agencies find desirable.

In practice, bike-sharing schemes are designed to fit existing transit systems, with little or no adjustments to the latter. Policy studies on the subject presume this separate approach to design (e.g. Cheng and Liu, 2012; Li and Loo, 2016; Muñoz et al., 2016). Empirical studies reflect this approach as well (e.g. Faghih-Imani et al., 2017; Ma et al., 2015; Martens, 2007; Midgley, 2009; Nadal, 2007; Yang et al., 2015).

To our knowledge, the literature remains silent on the subject of jointly designing shared bike systems with the transit trunk-line networks they feed. This is surprising, since the higher access and egress speeds of bicycles (relative to walking) might justify trunk-line designs with greater spacings between routes and stops. These could lower operating costs for the transit agency, as well as trip times for its patrons. Both advantages were found when transit

trunk networks were jointly optimized with feeder services furnished by buses (e.g. Chen and Nie, 2017a; Sivakumaran et al., 2014).

In light of the above, the present chapter explores (i) how shared-bike feeder systems might best be designed to fit existing (and unalterable) trunk-line transit networks; and (ii) how these same feeders and trunk networks might be optimized jointly. In both thrusts, shared bikes are accessed via docking stations. And in both thrusts, designs are optimized without the aid of discrete models of the kind in Ibarra-Rojas et al. (2015) and Kepaptsoglou and Karlaftis (2009), since these furnish solutions that are case-specific.

We opt instead to formulate and use parsimonious, continuous models in line with Newell (1971) and Wirasinghe and Ghoneim (1981). Doing so required a host of simplifying assumptions. Most pertain to travel demands, which are assumed to be uniformly distributed over our networks, and invariant to network designs. Though these may be viewed as controversial in some circles, all of the assumptions have been adopted in previous works; e.g. see (Chen et al., 2015; Daganzo, 2010a, b; Estrada et al., 2011; Fan et al., 2018; Sivakumaran et al., 2014). The advantage of our approach lies in the general insights that it produces.

Present insights pertain to both thrusts (i) and (ii) above, and were sharpened via parametric analyses. Our case studies collectively entail trunk networks that are served by ordinary buses, by bus rapid transit (BRT) and by metro rail. Each of these forms was explored under three feeder options in which patrons: walk to and from trunk stations sans other options; choose whether or not to ride fixed-route feeder buses; and choose instead whether to ride shared bikes. We further parse each combination of trunk and feeder system by varying the city's size, its travel demand, and its economic condition.

In all these many cases, the trunk-line networks conform to the hybrid structure proposed in Daganzo (2010a), and briefly reviewed in the following section. The continuous models formulated for the three feeder options are presented in the following section as well. Parametric analyses are presented in Section 2.3. Section 2.3 also explores how shared bikes can be priced so that transit agencies can always break even, with or without subsidies. Tailoring present findings to real-world environments is discussed in Section 2.4.

2.2 Models

Section 2.2.1 reviews ideas in Daganzo (2010a) for designing transit networks accessed on foot. Our reiteration of these ideas is kept to a minimum, and is offered to justify new ideas that follow. These come in Sections 2.2.2 and 2.2.3 and pertain to access via shared bicycles and feeder buses, respectively. A solution method is presented in Section 2.2.4. Notations used throughout this chapter are provided in Appendix A.1.

2.2.1 Accessing transit on foot

Consider the square-shaped city of size $D \times D$ (km^2) in Fig. 2.1 with a dense grid of streets throughout that are parallel to the city's boundaries. As per assumptions in Daganzo (2010a), Chang and Schonfeld (1991), and Medina et al. (2013), demand for transit travel: is exogenous and inelastic to transit service; has an hourly rate of λ_p (trips/h/km^2) during the peak period of duration t_p (h/day), a lower rate λ_o (trips/h/km^2) during the off-peak of duration t_o (h/day); and has origins and destinations that are uniformly distributed over the entire city. The average demand density $\lambda = \frac{\lambda_p t_p + \lambda_o t_o}{t_p + t_o}$ will be used as a proxy for the city's population density. The patrons' value of time, μ (\$/h), will serve as a proxy for the average hourly wage of city residents.

In further keeping with previous studies, a patron is assumed to: access and egress a transit system via the station nearest her origin and destination, respectively; arrive at her origin station randomly, regardless of the service schedule; choose the shortest-distance route; and choose between routes with equal probability, should multiple shortest routes exist. For simplicity, transit vehicles are assumed to stop at every station along a route, and dwell for time τ at each station.[1]

Transit routes collectively form the hybrid structure shown in Fig. 2.1 in bold. In a (shaded) central area of size $\alpha D \times \alpha D$ (where α is a decision variable), lines evenly spaced at S (km) form a grid. The lines extend (and branch as needed) in the periphery, with stations

[1] With modest additions, the model can treat the dwell time at each stop as a linear function of its boarding patrons, as in Daganzo (2010a); Estrada et al. (2011); and Fan et al. (2018).

again spaced at S. Vehicle headways in the central area are H_p (h) and H_o (h) during peak and off-peak times, respectively.

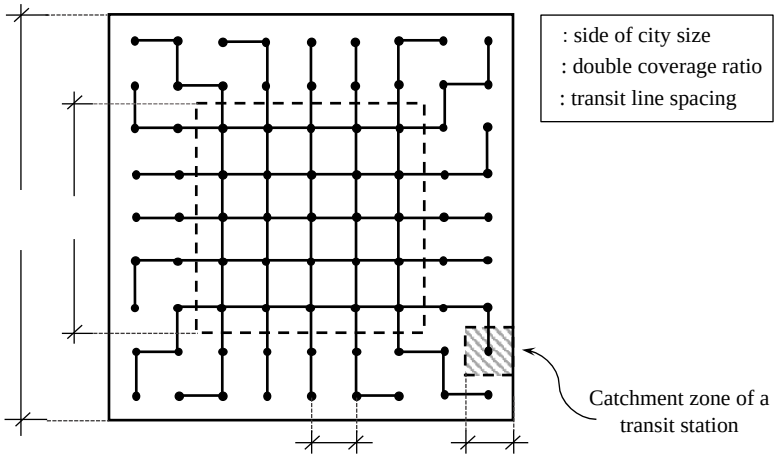

Fig. 2.1. A hybrid transit network atop a grid street network in a square city (Daganzo, 2010a).

In formulating the cost-minimization problem for this hybrid network, the costs born to patrons and the agency will be expressed in units of time (Chen and Nie, 2017a, b, 2018; Daganzo, 2010a, b), and with decision variables S, H_p, H_o, and α. The formulation is:

$$\min_{S,H_p,H_o,\alpha} \quad \frac{t_p\lambda_p(UC_{W,p}+AC_p)+t_o\lambda_o(UC_{W,o}+AC_o)}{t_p\lambda_p+t_o\lambda_o} \tag{2.1a}$$

$$\text{subject to:} \quad \lambda_k SDH_k \cdot \max\left\{\frac{1-\alpha^2}{2\alpha}, \frac{3+2\alpha^2-3\alpha^4}{8\alpha}+\frac{D(1-\alpha^2)^2}{32S}\right\} \le K,\ k\in\{p,o\} \tag{2.1b}$$

$$H_k \ge H_{min},\ k\in\{p,o\} \tag{2.1c}$$

$$S > 0 \tag{2.1d}$$

$$S/D \le \alpha \le 1, \tag{2.1e}$$

where $UC_{W,p}$ and $UC_{W,o}$ denote the patrons' average trip costs in peak and off-peak periods, respectively; and AC_p and AC_o are the average peak and off-peak trip costs incurred by the transit agency. Constraint (2.1b) ensures that the number of patrons onboard a transit vehicle never exceeds its passenger-carrying capacity, K, where the left-hand-side is the maximum onboard occupancy for period k; see Daganzo (2010a) for the derivation. Constraint (2.1c) prevents headways from falling below a minimum, H_{min}, as determined by safety

considerations or the system's vehicle-carrying capacity; and (2.1d) and (2.1e) are boundary constraints for the decision variables.

The patrons' average trip cost in period k is formulated as:

$$UC_{W,k} = \frac{S}{v_w} + E_{T,k},\ k \in \{p, o\} \tag{2.2a}$$

$$E_{T,k} = H_k\left(\frac{2+\alpha^3}{3\alpha} + \frac{\left(1-\alpha^2\right)^2}{4}\right) + \delta\left(1 + \frac{\left(1-\alpha^2\right)^2}{2}\right) + \frac{D}{12}\left(\frac{1}{v} + \frac{\tau}{S}\right)(12 - 7\alpha + 5\alpha^3 - 3\alpha^5 + \alpha^7),\ k \in \{p, o\} \tag{2.2b}$$

where v_w is walking speed, such that $\frac{S}{v_w}$ is the average time spent accessing and then egressing transit stations; δ is the penalty cost per transfer (in hours); v is the transit vehicle's cruise speed; and τ denotes the vehicle's dwell time at each station due to patrons' boarding and alighting behavior, and vehicle acceleration and deceleration. The $E_{T,k}$ is the sum of: (i) average wait time per trip at the origin and transfer stations in period k; (ii) average transfer penalty per trip; and (iii) average in-vehicle travel time per trip.

The average agency cost per trip in period k is formulated as:

$$AC_k = \frac{1}{\mu\lambda_k}\left(\$_I + \$_S + \$_{VD,k} + \$_{VT,k}\right),\ k \in \{p, o\}, \tag{2.3a}$$

where $\$_I$ denotes the amortized construction and maintenance cost for the transit line infrastructure; $\$_S$ the amortized construction and operating cost of transit stations; and $\$_{VD,k}$ and $\$_{VT,k}$ the distance-based transit operating cost (e.g. the fuel cost) and the time-based transit operating cost (e.g. the amortized vehicle purchase and maintenance cost, and staff wages), both in period k. The above four costs are expressed in the unit \$/h/km^2, and are converted to temporal cost per trip by dividing them by $\mu\lambda_k$. The four costs are formulated as:

$$\$_I = \frac{\left(1+\alpha^2\right)C_I}{S} \tag{2.3b}$$

$$\$_S = \frac{C_S}{S^2} \tag{2.3c}$$

$$\$_{VD,k} = \frac{2\left(3\alpha-\alpha^2\right)C_{VD}}{SH_k},\ k \in \{p, o\} \tag{2.3d}$$

$$\$_{VT,k} = \frac{2\left(3\alpha-\alpha^2\right)C_{VT}}{SH_k}\left(\frac{1}{v} + \frac{\tau}{S}\right),\ k \in \{p, o\}, \tag{2.3e}$$

where C_I, C_S, C_{VD}, C_{VT} are unit cost parameters: C_I (\$/h/km) denotes the amortized monetary cost per km of transit line per hour of operation; C_S (\$/h/station) the amortized cost per station per hour; C_{VD} (\$/km/vehicle) the unit distance-based operating cost; and C_{VT} (\$/h/vehicle) the unit time-based operating cost. In the interest of brevity, further explanation and derivation of (2.2a-b) and (2.3a-e) are omitted here. Readers can refer to Daganzo (2010a) for details.

Note that transit fare is not included in the generalized cost models, since it is simply a transfer of money from patrons to the agency.

2.2.2 Access via shared bikes

For the sake of simplicity, ignore the possibility that some travelers (e.g. those with short commutes) might use bicycles for their entire trips, and assume instead that shared bikes are used solely for accessing and egressing transit. The assumption is conservative because it over-estimates the costs incurred by some short-distance travelers, and therefore obscures the full benefits of shared-biking.

Our first order of business is to lay-out the docking stations where patrons check-out and return bicycles. Two types of stations are used: large docking stations that are placed next to transit stations to facilitate transit access and egress; and smaller docking stations that are uniformly distributed over a city at a density P (station/km^2). Layout of the latter stations is done per our first proposition below, with a proof relegated to Appendix B.

Proposition 2.1. For a given P, the diamond-grid layout of small docking stations shown in Fig. 2.2a (where the black dots represent the docking stations) minimizes the average walking distance between an average patron's origin or destination and the nearest docking station. The resulting average walking distance is $d_w = \sqrt{\frac{2}{9P}}$.

Note that when small docking stations are placed at the grid points of a diamond-grid layout, a station's catchment zone has a diamond shape as shown in Fig. 2.2b. The average access distance is equal to the L_1-distance (Manhattan distance) between the docking station and the centroid of the shaded triangle (i.e. a quarter of the catchment zone) in the figure. One can easily verify that this average access distance is $\sqrt{\frac{2}{9P}}$. (Recall that the streets are parallel to the city's boundaries.)

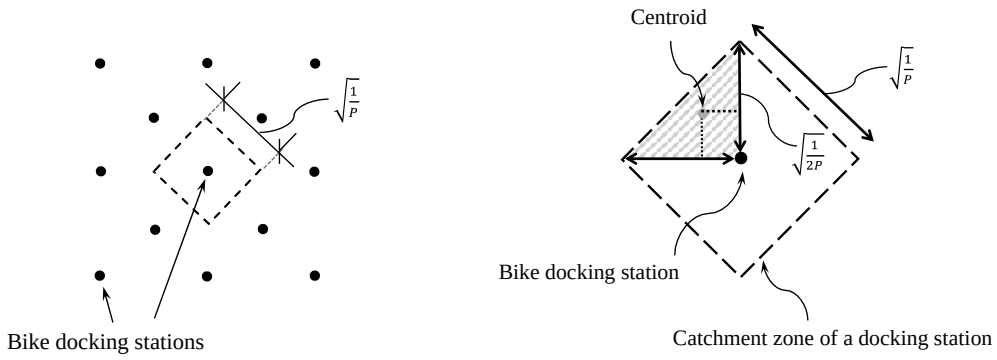

(a) (b)

Fig. 2.2. The optimal layout of small bike docking stations.

The joint optimization of the transit network and docking stations takes five decision variables and is formulated as follows:

$$\min_{S,H_p,H_o,\alpha,P} \quad \frac{t_p\lambda_p(UC_{B,p}+AC_p)+t_o\lambda_o(UC_{B,o}+AC_o)}{t_p\lambda_p+t_o\lambda_o} + AC_B \tag{2.4}$$

subject to: (2.1b-e) and $P \geq 0$,

where $UC_{B,k}$ ($k \in \{p, o\}$) denotes the average patron's cost in period k; and AC_B the bike-sharing agency cost per trip, to be defined in due course. The AC_k ($k \in \{p, o\}$) is the same as defined in (2.3a-e). The new patron cost, $UC_{B,k}$ is given by:

$$UC_{B,k} = E_{B,k} + E_{T,k}, \text{for } k \in \{p, o\}. \tag{2.5}$$

where a trip's average access and egress time by walking, $\frac{S}{v_w}$ in (2.2a), is replaced in (2.5) by $E_{B,k}$ to account for the costs of cycling, and $E_{T,k}$ ($k \in \{p, o\}$) is the same as defined in (2.2b).

The bike-sharing agency cost, AC_B is formulated as:

$$AC_B = \frac{C_P\cdot\left(P+\frac{1}{S^2}\right)+(C_B+\xi C_D)\frac{n_B\lambda_p}{\rho}}{\mu(\lambda_p t_p+\lambda_o t_o)}, \tag{2.6}$$

where C_P (\$/station/day) denotes the fixed cost rate for the purchase, installation, and maintenance of a docking station, amortized over its lifecycle. For simplicity, we use the same unit cost rate for both large docking stations deployed near transit stations, and small docking

stations distributed evenly over the city.[2] We denote C_B (\$/bike/day) and C_D (\$/dock/day) as the purchase, maintenance, and operating costs for each bike and each dock, respectively. These costs are amortized over the lifecycles of a bike and a dock. Further denote ξ as the fixed ratio between the numbers of docks and bikes for a bike-sharing system, which usually takes a value of 1.5~1.7 for real-world business solutions (Gauthier et al., 2013; Gleason and Miskimins, 2012; Tang et al., 2011; Yang et al, 2015). We specify $\frac{n_B \lambda_p}{\rho}$ as the number of bikes needed per km^2 of service area. The n_B denotes the average bike-hours used per patron during peak periods, depending on the proportion of the cycling region and the average time that a bike user occupies a bike in peak periods. Parameter ρ denotes the bikes' peak-period utilization ratio, i.e., the average proportion of time when a bike is in use during peak periods ($0 < \rho \leq 1$). The ρ indicates how fast the bikes are circulated during peak hours, which is affected by the demand imbalance, randomness, and the performance of bike redistribution strategies. When $\rho = 1$, each bike will be checked out immediately after someone returns it to a docking station, as may occur when the incoming and outgoing demands at each station are perfectly balanced and deterministic. Low values of ρ can be used to represent cases where the incoming and outgoing demands are highly stochastic and imbalanced between stations, and where no efficient bike redistribution strategy is implemented. Using low values of ρ would be conservative because more bikes and docks are needed to satisfy the demand, entailing a higher agency cost. For simplicity, detailed modeling of the bike redistribution strategy is omitted in this thesis, and its cost is assumed to be factored into the amortized costs for the bikes and the stations (Gleason and Miskimins, 2012; Wang, 2013b; Yang et al., 2015).

The derivation of $E_{B,k}(k \in \{p, o\})$ in (2.5) and n_B in (2.6), depend on how patrons choose between walking and renting shared bikes. To model these choices, we assume that only a certain proportion, β, of transit patrons are able-bodied and thus consider biking as a feeder option. These patrons choose between walking and cycling so as to lower their costs. The β reflects patrons' willingness to cycle, and can also be used to capture the long-term

[2] The size of each docking station can be determined from the proportion of incoming and outgoing bike flows. When space is limited, large docking stations can be designed as underground bike parking facilities, as in the Netherlands (Bicycle Dutch, 2018).

effects of weather, terrain and the presence or absence of bike-friendly facilities and policies.[3] The remaining $(1-\beta)$ of patrons access transit solely by walking (Nurworsoo et al., 2012).

Consider an able-bodied patron in period $k \in \{p, o\}$. Define d $(0 \le d \le S)$ as the access distance from that patron's origin to her nearest transit station, or as the egress distance between the patron's destination and the transit station nearest that destination.[4] Access or egress cost by riding a shared bike, $u_{Bk}(d)$, or by solely walking, $u_{Wk}(d)$, are formulated as:

$$u_{Bk}(d) = \frac{d}{v_b} + t_w + t_{dp} + t_{dd} + t_f + \frac{\varphi_k(d)}{\mu} \tag{2.7a}$$

$$u_{Wk}(d) = \frac{d}{v_w}, \tag{2.7b}$$

where v_b denotes the cycling speed; t_w the walking time from the patron's origin to the nearest bike station (from Proposition 2.1, we have $t_w \approx d_w/v_w = \frac{\sqrt{\frac{2}{9P}}}{v_w}$); t_{dp} and t_{dd} the times for picking-up and dropping-off a bike at a docking station, respectively; t_f the intermodal transfer penalty between the transit station and the nearby bike station; and $\varphi_k(d)$ the distance-based bike rental fee in period k. We present the following proposition concerning a patron's choice of access or egress mode.

Proposition 2.2. At system optimum, there exists a critical distance $d_{ck} > 0$ for each period $k \in \{p, o\}$, such that if a patron's access or egress distance $d < d_{ck}$, she will choose to walk to or from the transit station, and if an able-bodied patron's access or egress distance $d > d_{ck}$, she will choose to ride a shared bike.

Consider an able-bodied patron whose access distance is d $(0 \le d \le S)$. The marginal generalized cost to the system when the patron switches from walking to cycling is:

$$MC_{B-W} = \left(\frac{d}{v_b} + t_w + t_{dp} + t_{dd} + t_f + \frac{MAC_B}{\mu}\right) - \frac{d}{v_w}, \tag{2.8a}$$

---

[3] More detailed choice models, such as probit or logit (Hausman and Wise, 1978; Taylor and Mahmassani, 1996; Wen and Koppleman, 2001) can be incorporated into our modeling framework too.

[4] An able-bodied patron may choose to ride a shared bike to access transit, or to egress transit, or to do both.

where $\frac{d}{v_b} + t_w + t_{dp} + t_{dd} + t_f$ is the patron's access time by bike; and MAC_B denotes the marginal bike-sharing agency cost (in \$) for serving this additional patron. The MAC_B is formulated as:

$$MAC_B = \begin{cases} (C_B + \xi C_D)\frac{1}{\rho \cdot t_p}\left(\frac{d}{v_b} + t_{dp} + t_{dd}\right), & \text{for a peak-period patron} \\ 0, & \text{for an off-peak-period patron.} \end{cases} \quad (2.8b)$$

Recall that ρ is the bike utilization ratio during peak periods. Thus, $\frac{1}{\rho \cdot t_p}\left(\frac{d}{v_b} + t_{dp} + t_{dd}\right)$ is the number (fraction) of bikes the additional cycling patron occupies during peak hours. The marginal bike-sharing agency cost is zero during off-peak hours because there are always redundant bikes.

Note now that MC_{B-W} is a linear function of d. Thus, the equation $MC_{B-W} = 0$ has a unique solution of d for each $k \in \{p, o\}$. We denote this solution as d_{ck} (the critical distance) for period k, and have:

(i) if $d < d_{ck}$, then $MC_{B-W} > 0$, and thus the able-bodied patron will choose to walk to or from the nearest transit station;

(ii) if $d > d_{ck}$, then $MC_{B-W} < 0$, and the able-bodied patron will choose to rent a bike; and

(iii) if $d = d_{ck}$, then $MC_{B-W} = 0$, and the able-bodied patron is indifferent between walking and riding a shared bike. ■

The critical distance, d_{ck} $(k \in \{p, o\})$, can be derived by solving the equation $MC_{B-W} = 0$. The detailed derivation is furnished in Appendix C.

Following Proposition 2.2, denote the part of a catchment zone that is defined by $d < d_{ck}$ as the "walk-only" region, and the remaining catchment zone as the "cycling" region. Only the able-bodied patrons originating in or destined for the cycling region will access or egress transit via shared bikes. The rest of the patrons will choose walking. The isodistance lines at d_{ck} $(k \in \{p, o\})$ may or may not reach the boundaries of a transit station's catchment area. Depending on the value of $\frac{d_{ck}}{S}$, the walk-only region can take one of the three shapes as shown in Fig. 2.3a-c. In each figure: the black dot represents the transit station; the solid lines are the

isodistance lines at d_{ck}; the dashed lines are the boundary of the catchment zone; and the walk-only region is marked by shading.

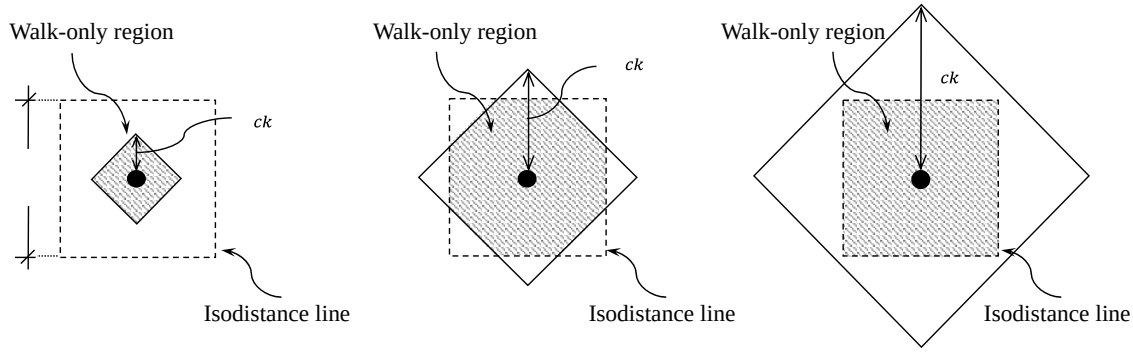

(a) when $\frac{d_{ck}}{S} \leq \frac{1}{2}$; (b) when $\frac{1}{2} < \frac{d_{ck}}{S} < 1$; (c) when $\frac{d_{ck}}{S} \geq 1$.

Fig. 2.3. The walk-only region in the catchment zone of a transit station in period $k \in \{p, o\}$.

For each of the three cases shown in Fig. 2.3a-c, we define $A_{bw,k}$ as the area of the walk-only region in period k, $d_{bin,k}$ as the average access distance for the origins and destinations in the walk-only region, and $d_{bout,k}$ as the average access distance in the cycling region in period k. The $E_{B,k}$ can be calculated by averaging the access and egress costs for the walkers and the cyclists. We then have the following corollary of Proposition 2.2:

Corollary 2.1. The $E_{B,k}$ under the system-optimal choices of access modes is given by:

$$E_{B,k} = (1-\beta)\frac{S}{v_w} + 2\beta\left(\frac{A_{bw,k}}{S^2}\cdot\frac{d_{bin,k}}{v_w} + \left(1-\frac{A_{bw,k}}{S^2}\right)\left(\frac{d_{bout,k}}{v_b} + t_w + t_{dp} + t_{dd} + t_f\right)\right), k \in \{p, o\} \quad (2.9)$$

The derivations for $A_{bw,k}$, $d_{bin,k}$ and $d_{bout,k}$ are relegated to Appendix C.[5] The average bike-hours used per peak-period patron, n_B, can be calculated as $n_B = 2\beta\left(1-\frac{A_{bw,k}}{S^2}\right)\left(\frac{d_{bout,k}}{v_b} + t_{dp} + t_{dd}\right)$.

We further present the following proposition, with a proof relegated to Appendix D.

[5] A similar method was used in Chen and Nie (2017a) for the access mode assignment between walking and riding via a flexible-route feeder service.

Proposition 2.3. The above system optimum can be attained by appropriately pricing the bike rental fee.

Appendix D also presents a scheme that entails the system optimum mode choices, in which the bike rental fee increases linearly with distance. Note that although the bike rental fee affects a patron's choice to walk or cycle, this fee is not a part of the generalized cost because it is a transfer of money from the bike users to the operating agency.

2.2.3 Access via fixed-route feeder buses

Consider the trunk and fixed-route feeder-bus network proposed in Sivakumaran et al. (2014), and shown in Fig. 2.4. The large, dark circle is a transit trunk station with a catchment zone bounded by dashed lines. The thick solid lines represent trunk lines as they would be laid-out in a grid network. (Note that in the peripheral area of a hybrid trunk-line network, only part of the two trunk lines shown in Fig. 2.4 may exist). The thinner solid lines with arrowheads (shown for illustration in the lower-right portion of the catchment zone) are feeder-bus lines. The small squares are feeder-bus stops.

We use the continuous cost model formulated in Sivakumaran et al. (2014) to design the trunk and feeder network, but with two modifications. These (i) accommodate the hybrid trunk network previously shown in Fig. 2.1; and (ii) enable transit patrons to choose between walking and riding a feeder bus to and from trunk stations. The formulation has seven decision variables ($S, H_p, H_o, \alpha, S_f, H_{f,p}, H_{f,o}$) and takes the form:

$$\min_{S,H_p,H_o,\alpha,S_f,H_{f,p},H_{f,o}} \quad \frac{t_p\lambda_p\left(UC_{F,p}+AC_p+AC_{F,p}\right)+t_o\lambda_o\left(UC_{F,o}+AC_o+AC_{F,o}\right)}{t_p\lambda_p+t_o\lambda_o} \tag{2.10a}$$

subject to:

$$\frac{\left(1-\frac{A_{fw,k}}{S^2}\right)\cdot\lambda_k\cdot S_f\cdot S\cdot H_{f,k}}{4} \le K_f, \quad k \in \{p,o\} \tag{2.10b}$$

$$H_{f,k} \ge H_{fmin}, \quad k \in \{p,o\} \tag{2.10c}$$

$$S_f > 0 \tag{2.10d}$$

$$\frac{S}{S_f} \in \{1,2,3,\dots\} \tag{2.10e}$$

(2.1b-e),

where $UC_{F,k}$ is the patrons' average trip cost for period k; $AC_{F,k}$ is the agency cost for feeder-bus service; $A_{fw,k}$ is the area within a trunk station's catchment zone where patrons access and

egress trunk service on foot (see Appendix F for the derivation); $H_{f,k}$ is the feeder-bus headway; S_f is the spacing between feeder-bus lines and stops, which are assumed equal for simplicity; K_f is a feeder bus's passenger-carrying capacity; and H_{fmin} is the minimum headway for a feeder-bus line. The agency cost for trunk-line service in period k, AC_k ($k \in \{p, o\}$), is the same as in (2.3a-e). Constraint (2.10b) reflects the limits in feeder-bus carrying capacity, where the left-hand-side is the maximum number of onboard passengers allowed for period k. Constraint (2.10c) specifies the minimum headway for feeder buses. Constraint (2.10e) requires trunk line spacing to be an integer multiple of feeder line spacing.

The user cost for feeder-bus service, $UC_{F,k}$, is formulated as:

$$UC_{F,k} = E_{F,k} + E_{T,k},\ k \in \{p, o\}, \tag{2.11}$$

where $E_{F,k}$ is the average access and egress cost per trip for period k. The $E_{F,k}$ depends on how patrons choose between walking and riding a feeder bus, and is derived in a manner similar to $E_{B,k}$ in Section 2.2.2. The detailed derivation is relegated to Appendix E.

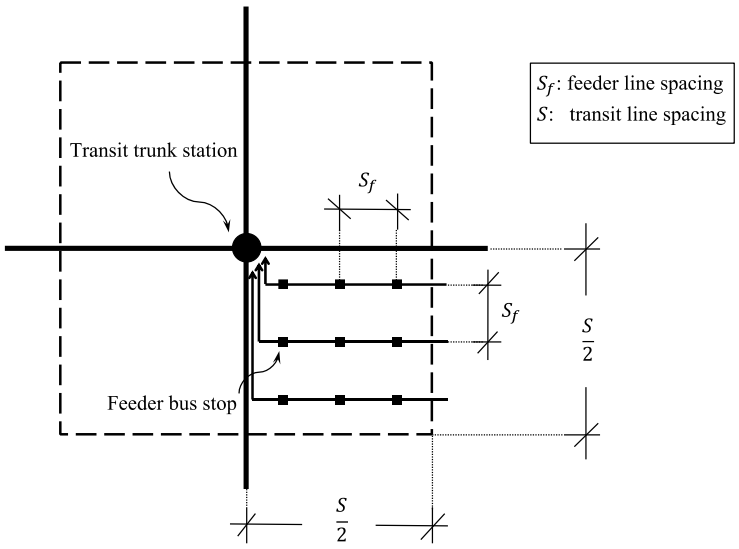

Fig. 2.4. The feeder bus network in Sivakumaran et al. (2014).

The feeder agency cost, $AC_{F,k}$ ($k \in \{p, o\}$), is formulated as:

$$AC_{F,k} = \frac{1}{\mu \lambda_k S_f}\left(C_{fI} + \frac{C_{fS}}{S_f} + \frac{3C_{fVD}}{H_{f,k}} + \frac{C_{fVT}}{H_{f,k}}\left(\frac{3}{v_f} + \frac{2\tau_f}{S_f}\right)\right),\ k \in \{p, o\}, \tag{2.12}$$

where C_{fI} (\$/h/km) denotes the amortized hourly cost per km of feeder line infrastructure; C_{fS} (\$/h/stop) the amortized hourly cost for constructing and maintaining a feeder bus stop; C_{fVD} (\$/km/bus) and C_{fVT} (\$/h/bus) are the unit distance-based and time-based feeder bus operating costs, respectively; v_f the cruise speed of feeder buses; and τ_f the feeder bus dwell time at a stop. Refer to Sivakumaran et al. (2014) for the derivation of (2.12).

2.2.4 Solution method

We first derive the closed-form optimal solution for trunk-line headway, H_k $(k \in \{p, o\})$, in (2.1), (2.4) and (2.10). The solution is the same for these three mathematical programs because the parts of their objective functions and the constraints related to H_k are the same for all three. All three programs are convex in H_k, and when the constraints are ignored the first-order condition with respect to H_k yields:

$$\widetilde{H}_k = \sqrt{\frac{2(3\alpha-\alpha^2)\left[C_{VD}+C_{VT}\left(\frac{1}{v}+\frac{\tau}{S}\right)\right]}{\mu\lambda_k S\left(\frac{2+\alpha^3}{3\alpha}+\frac{(1-\alpha^2)^2}{4}\right)}},\ k \in \{p, o\}. \tag{2.13}$$

Constraints (2.1b-c) specify that H_k is bounded from above and below by $\frac{K}{\lambda_k SD \cdot \max\left\{\frac{1-\alpha^2}{2\alpha}, \frac{3+2\alpha^2-3\alpha^4}{8\alpha}+\frac{D(1-\alpha^2)^2}{32S}\right\}}$ and H_{min}, respectively. Thus, the closed-form solution for H_k can be written as a function of α and S as follows:

$$H_k^* = \text{mid}\left(\widetilde{H}_k, H_{min}, \frac{K}{\lambda_k SD \cdot \max\left\{\frac{1-\alpha^2}{2\alpha}, \frac{3+2\alpha^2-3\alpha^4}{8\alpha}+\frac{D(1-\alpha^2)^2}{32S}\right\}}\right),\ k \in \{p, o\}, \tag{2.14}$$

where the function $\text{mid}(\cdot)$ takes the middle value among the three arguments.

With (2.14), the number of decision variables is reduced to: two for walk-only access (S, α); three for bike-sharing access (S, α, P); and five for feeder-bus access $(S, \alpha, S_f, H_{f,p}, H_{f,o})$. Thanks to the small number of decision variables, these reduced

optimization models can be solved by a number of commercial solvers. We employ the "fmincon" tool with the sequential quadratic programming algorithm in MATLAB R2016b.[6]

The above method cannot guarantee a globally-optimal solution, owing to the non-convex nature of the programs. Thus, we repeated the procedure 10 times for each case study examined in the chapter. Each time the optimization started with an initial solution randomly selected from the feasible ranges of decision variables, which were defined as: $S \in [0.05, 2.5]$ km, $\alpha \in \left[\frac{S}{D}, 1\right]$, $P \in [10, 1000]$ station/km^2, $S_f \in [0.05, 0.5]$ km, and $H_{f,p}, H_{f,o} \in \left[\frac{1}{60}, \frac{1}{3}\right]$ h. We found that each repetition of the solution procedure always produced the same final solution, and are therefore confident in our solution.

2.3 Numerical analyses

Parameter values used in our numerical tests are presented in Section 2.3.1. Feeder systems are designed to suit pre-existing transit networks in Section 2.3.2. Trunk and feeder systems are optimized jointly in Section 2.3.3. We examine how bike-sharing fees can ensure that agencies break even on fare revenues and costs in Section 2.3.4.

2.3.1 Parameter values

We borrow from Daganzo (2010a) and Chen et al. (2015) and specify that the square city's length (and width), $D \in [10, 30]$ km; demand density, $\lambda \in [200, 3000]$ trips/h/km^2; peak-period duration, $t_p = 4$ h; off-peak duration, $t_o = 14$ h; and $\lambda_p = 2.5\lambda$. A low walking speed, $v_w = 2$ km/h is used to account for delays at street junctions and for the inconvenience of walking (Daganzo, 2010a). A value of time $\mu = 5$ \$/h is used for low-wage cities, and $\mu = 25$ \$/h for high-wage ones.

Cost and operating parameters for ordinary buses, BRT and metro rail trunk-line systems are furnished in Table 2.1. These are borrowed from Daganzo (2010a), Gu et al. (2016),

[6] We solve the program for feeder-bus access by first ignoring the integer constraint (2.10e). If in the solution $\frac{S}{S_f} = \kappa$ is not an integer, we specify that $\frac{S}{S_f}$ equals each of κ's two neighboring integers; separately solve the programs for both integer neighbors; and take the lower-cost solution to be optimal (see Chen and Nie, 2017a; Fan et al., 2018; Nourbakhsh and Ouyang, 2012).

Sivakumaran et al. (2014) and Fan et al. (2018). The C_{VT}, C_I, and C_S are formulated as linear functions of wage rate, μ, to capture labor costs; see Gu et al. (2016) for details.

Table 2.1. Operating and cost parameters for three transit technologies: bus, BRT, and rail.

	Operating Parameters						**Cost Parameters**			
							Operating cost rates		Infrastructure cost rates	
	τ (s)	t_f (s)	v (km/h)	δ (h)	K (passenger /veh)	H_{min} (min)	C_{VD} ($/km)	C_{VT} ($/h)	C_I ($/h/km)	C_S ($/h/station)
Bus (including feeder bus)	30	30	25	0.015	80	1	0.59	$2.66 + 3\mu$	$6 + 0.2\mu$	$0.42 + 0.014\mu$
BRT	30	30	40	0.015	160	1	0.66	$3.81 + 4\mu$	$162 + 5.4\mu$	$4.2 + 0.14\mu$
Rail	45	60	60	0.1	3000	1.5	2.20	$101 + 5\mu$	$594 + 19.8\mu$	$294 + 9.8\mu$

Values for C_B, C_D and C_P are furnished in Table 2.2 for bike-sharing systems in low- and high-wage cities. These cost rates are derived in Appendix F. Table 2.2 also presents the values used for t_{dp}, t_{dd}, v_b, and ξ, along with two values for β to represent walk- and bike-friendly cities, and two values for ρ to reflect low and high bike utilizations. All values were taken from the literature, as cited in the table.

Table 2.2. Operating and cost parameters for bike-sharing systems.

Operating Parameters							
t_{dp} (s)	t_{dd} (s)	v_b (km/h)	$\xi^{\#}$	$\beta^{※}$		$\rho^{§}$	
				Low (walk-friendly)	High (bike-friendly)	Low bike utilization	High bike utilization
30	30	12	1.5	0.3	0.5	0.3	0.5
Cost Parameters							
C_B ($/bike/day)				C_D ($/dock/day)		C_P ($/station/day)	
Low-wage	High-wage			Low-wage	High-wage	Low-wage	High-wage
0.44	2.58			0.08	0.65	9.36	19.10

[#] This value is taken from Gleason and Miskimins (2012).

[※] The two values of β are selected according to the bicycle ownership and mode share data in Gunn (2018) and Oke et al. (2015).

[§] The two values of ρ are selected conservatively by referring to the empirical data of bike usage found in Hampshire and Marla (2012), Lane (2015) and Suzuki and Nakamura (2017).

We devised a large set of case studies by endowing cities with the eight possible combinations of μ, β and ρ. Each of these eight city types was separately served by ordinary

buses, BRT and metro rail. In separate analyses, the first of these trunk-line systems was accessed and egressed by walking (only) and by riding shared bikes. The latter two trunk-line systems were separately fed by all three options (walking, riding bikes and riding feeder buses). These 64 combinations were separately examined under ranges of D and λ.

2.3.2 Pre-existing transit service

We explore whether shared-bikes or feeder-buses can reduce the costs of existing transit systems. Trunk-line networks are optimized to serve access on foot; i.e., the S, α, and H_k $(k = p, o)$ are obtained by solving (2.1). The resulting lines and stations are assumed to be immovable. This gives foot-access an advantage when drawing comparisons against the two other feeder options. For the shared-bike option, the density of small docking stations, P, is optimized by solving (2.4) when S, α, and H_k are fixed and determined by (2.1). The S_f, α and $H_{f,k}$ $(k = p, o)$ are optimized for feeder-bus service using (2.10) in similar fashion.

Consider first cities with a high wage of $\mu = 25$ \$/h, and that are more favorable to walking than to biking, such that $\beta = \rho = 0.3$. We find that shared-bikes can reduce generalized costs in most cases when transit service is provided by ordinary buses, save for those where D and λ are both high. The contour lines in Fig. 2.5a show the percent reductions in costs for wide ranges of D and λ. Given our choices for β and ρ, the savings are modest and never reach 3%. They diminish as D or λ increases. This is because the transit vehicle capacity constraint (2.1b) is binding, and thus the optimal line and stop spacing, S, decreases as D or λ grows. The shorter-spaced transit stations are better accessed via walking; see the top-right corner demarcated by the boldface contour line in the figure.

Shared-bike access was also found to produce lowest costs for a greater range of D and λ when trunk-line services in these cities were provided by BRT. Fig. 2.5b shows that shared bikes result in lower costs than does walk-only access, save for the top-right corner, which is again demarcated by a boldface contour line. These savings are slightly greater than those when trunk-line transit service is provided by buses, because a BRT network has greater line and

stop spacings than does a bus network under the same demand level, which favors access by bike.[7]

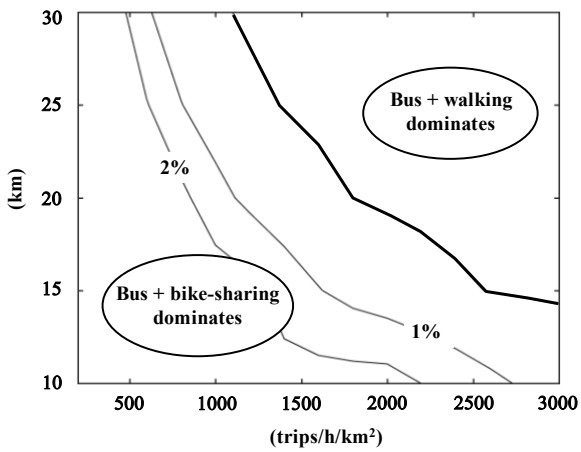

(a) pre-existing ordinary bus networks

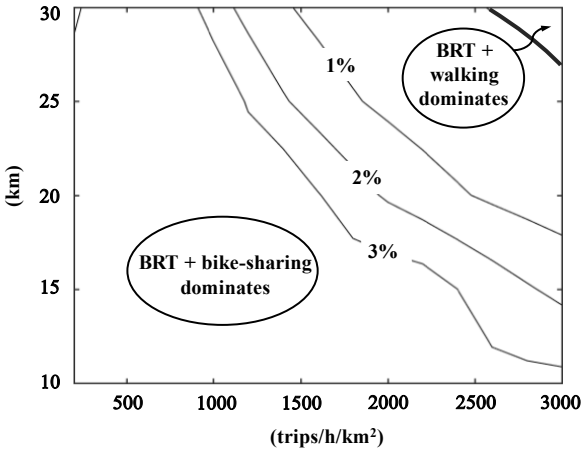

(b) pre-existing BRT networks

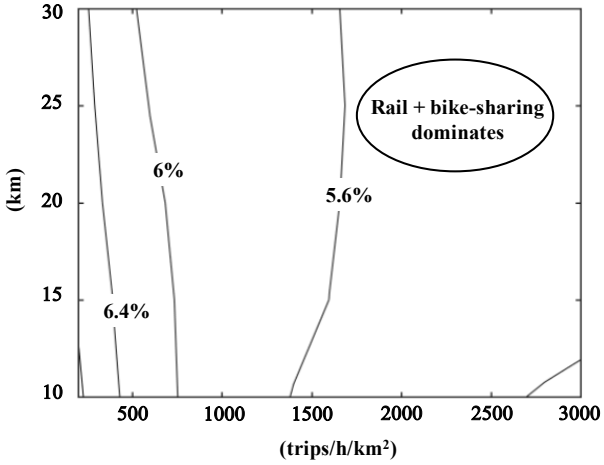

(c) pre-existing metro-rail networks

Fig. 2.5. Percentage savings in generalized costs by adding share-bikes or feeder-buses to fit pre-existing transit networks in high-wage, walk-friendly cities with low bike utilization ($\mu =$ 25 \$/h, $\beta = \rho = 0.3$).

[7] Before the capacity constraint becomes binding, the cost saving would increase with D. This is because longer trips in big cities require larger spacings between BRT lines and stations, which are better accessed by fast-moving bikes. This was observed when $D \leq 10$ km, which is not shown in Fig. 2.5b.

Shared-bike access is invariably the lowest-cost means when trunk-line service is provided by rail. Thanks to the large line and station spacings required of rail, the cost savings brought by adding bikes can exceed 6%; see Fig. 2.5c. In all three figures, feeder-bus access is never the lower-cost option.

Shared bikes can produce greater cost savings in low-wage cities. This becomes clear by visually comparing Fig. 2.6a with Fig. 2.5b. Savings grow to over 7% when circumstances are friendlier to cycling; i.e., under higher values of β and ρ. This becomes clear by comparing Fig. 2.6b with Fig. 2.5b.

2.3.3 Systems designed from scratch

Generalized costs diminished when trunk and feeder systems were optimally designed in joint fashion. When trunk services were provided by ordinary buses and BRT, shared bikes continued to be a lower-cost feeder option than walking for the majority of the D and λ examined. The cost savings were slightly greater as compared against those estimated in Section 2.3.2. This was true for both low- and high-wage cities. Of note, in jointly-optimized designs, substantial savings were often achieved in the agency cost of transit service due to the increased transit line and station spacings. The transit agency cost savings can offset a large portion (and sometimes all) of the added agency cost for providing the bike-sharing service.

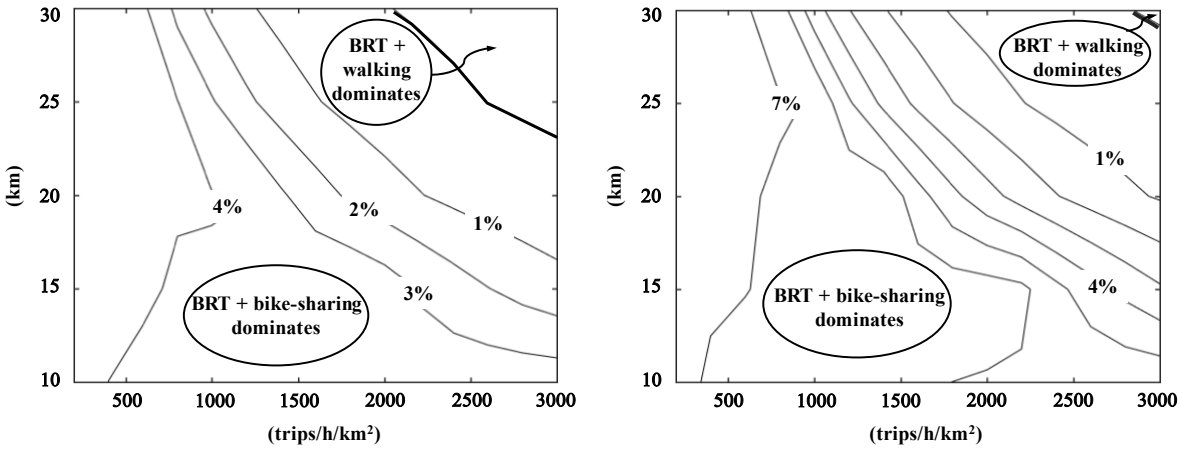

(a) low-wage, walk-friendly cities with low bike utilization ($\mu = 5$ \$/h, $\beta = \rho = 0.3$)

(b) high-wage, bike-friendly cities with high bike utilization ($\mu = 25$ \$/h, $\beta = \rho = 0.5$)

Fig. 2.6. Percentage savings in generalized costs by adding shared-bikes to feed existing BRT networks.

When trunk services were instead provided by rail, however, feeder buses become the lowest-cost option in most cases studied. Shared-bike access wins only when D and λ are both small; see Fig. 2.7. Higher-speed buses better suit the larger line and station spacings that metro-rail engenders. And economies of trip density are enjoyed by focusing higher demands onto those buses. Cost savings were substantial relative to access by walking; e.g. differences reached 20% for large D. As a practical matter, however, bike sharing might still be judged a preferred feeder option, since it imparts a lower cost to transit agencies.

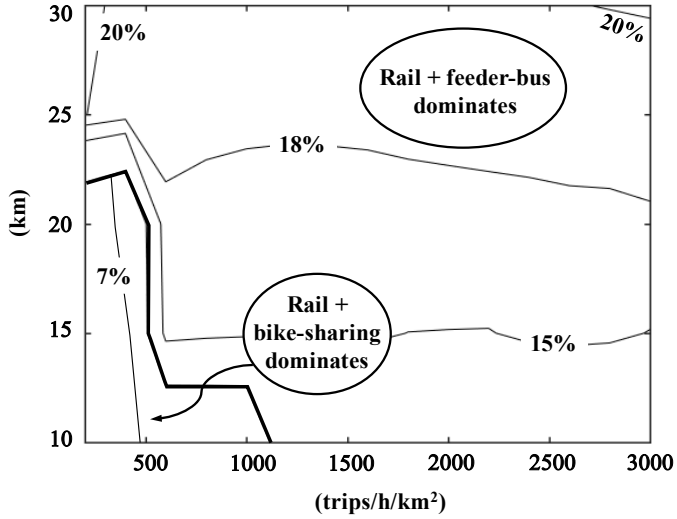

Fig. 2.7. Percentage savings in generalized costs for jointly-optimized metro-rail systems in high-wage, walk-friendly cities with low bike utilization ($\mu = 25$ \$/h, $\beta = \rho = 0.3$).

We think it of further interest to examine how D and λ affect lowest-cost designs when all 8 combinations of trunk and feeder options are in play. To this end, Fig. 2.8a and 2.8b show outcomes for low- and high-wage cities that are not especially favorable to cycling; i.e., we set $\beta = \rho = 0.3$. The contour lines demarcate cases in which certain trunk-feeder combinations produced the lowest generalized costs among all 8 options.

Tellingly, access by walking is never the winner. Nor are rail and shared-bike combinations preferred. Fig. 2.8a and 2.8b show instead that ordinary buses and BRT fed by shared bikes are the low-cost options in smaller, less-populated cities. In large cities with high demand density, metro-rail fed by buses produces the lowest cost. BRT and rail as trunk options are more favorable in rich cities where patrons place a higher premium on their time.

2.2.4 Break-even fee schemes for the bike-sharing system

We now examine how bike-sharing fees can ensure that agencies break even on fare revenues and costs in this section; i.e., how revenues generated by bike-sharing feeder systems can match their costs under system-optimal conditions. To look for insights, we continue to assume that travel demand, λ, is exogenous to features of our trunk and feeder services; and focus on two piecewise-linear distance-based fee rates in (D4) of Appendix D. These rates are γ_p and γ_o (\$/km) for peak and off-peak periods, respectively. We assume that transit trunk and bike-sharing feeder systems are jointly optimized, and examine cases in which the cost savings brought by bike sharing are, and are not, used to subsidize feeder service. In both cases, bike-rental revenue, R (\$/day/km^2), is calculated as:

$$R = \beta\left(\lambda_p t_p \oiint_{d\sigma\in A_{b,p}} \varphi_p(d;\gamma_p)d\sigma + \lambda_o t_o \oiint_{d\sigma\in A_{b,o}} \varphi_o(d;\gamma_o)d\sigma\right), \tag{2.15}$$

where: the two surface integrals in parentheses are integrated over the cycling regions, $A_{b,p}$ and $A_{b,o}$ (see Appendix E), and $\varphi_p(d;\gamma_p)$ and $\varphi_o(d;\gamma_o)$ are given by (D4).

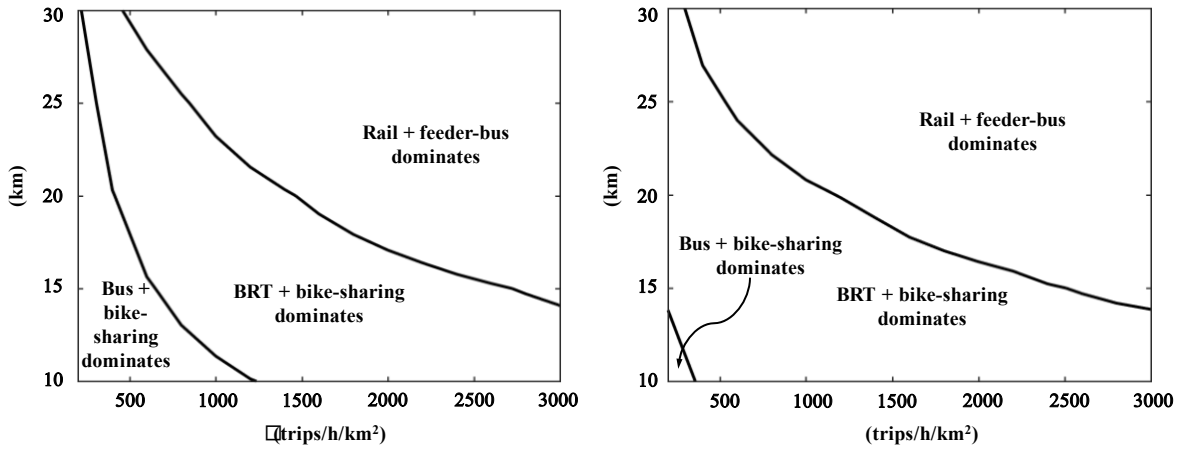

(a) low-wage cities with $\mu = 5$\$/h (b) high-wage cities with $\mu = 25$\$/h

Fig. 2.8. Lowest-cost designs for walk-friendly cities with low bike utilization ($\beta = \rho = 0.3$).

In the absence of subsidies, the system-optimal range of (γ_p, γ_o) is given by $0 \le \gamma_p, \gamma_o < \mu\left(\frac{1}{v_w} - \frac{1}{v_b}\right)$; see Appendix D. This range is plotted as a rectangle in Fig. 2.9 for a low-wage city with $\mu = 5$ \$/h that is small ($D = 10$ km) and walk-friendly ($\beta = \rho = 0.3$), and has trunk service provided by BRT. The break-even fee schemes are plotted as dashed, solid and

dotted lines for the λ shown in the figure's legend. For a given λ, the agency can presumably reap a profit by pricing the bike-sharing service at a point above the corresponding break-even line, and suffer a loss by setting the fee below that line.

Interestingly, the figure shows that break-even fees increase as λ grows. This is because optimal spacings between trunk stations decrease under larger λ, and the mode share for bikes diminishes owing to the smaller access and egress distances. Similarly, since trunk-station spacings increase with diminishing μ, break-even fees decrease accordingly. In contrast, break-even fees for small, high-wage cities could be unacceptably high, especially in walk-friendly cities with small β and ρ and in those with large λ. Figures for these results are not shown for brevity.

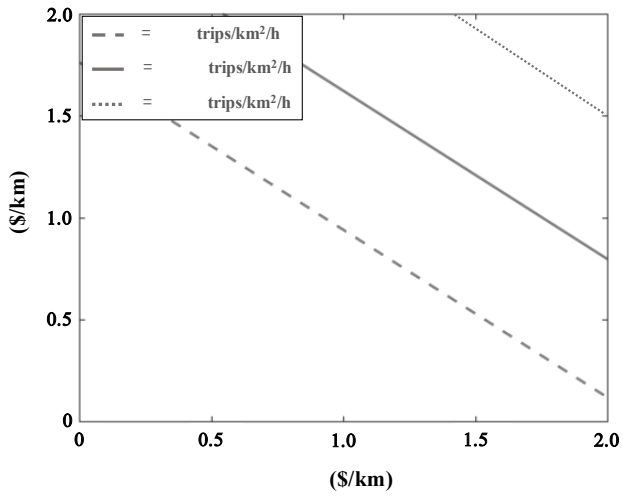

Fig. 2.9. Feasible ranges of break-even bike-rental fees for BRT trunk-feeder systems in a low-wage, small, walk-friendly city with low bike utilization ($\mu = 5$ \$/h, $D = 10$ km, $\beta = \rho = 0.3$)

Break-even fees diminish in the presence of subsidies. In these cases, we find that the entire system-optimal range of (γ_p, γ_o) is profitable in nearly all cases studied. Bike-rental fees can thus be set as low as a fixed rate $\varphi_p(d) = \frac{C_B + \xi C_D}{\rho t_p}\left(\frac{d_{cp}}{v_b} + t_{dp} + t_{dd}\right)$ during the peak periods, and $\varphi_o(d) = 0$ during the off-peak. (The former entails only \$0.023 per bike trip in a low-wage, walk-friendly, small city with low bike utilization, $D = 10$ km and $\lambda = 2000$ trips/h/km^2.) Those lowest fees are obtained by setting $\gamma_p = \gamma_o = 0$ in (D4), though details of this are omitted from the present thesis again in the interest of brevity.

2.4 Summary

A battery of tests has revealed that shared bikes can be a cost-effective means to access or egress public transit. When designed to fit pre-existing transit networks, shared-bike feeder systems reduced generalized costs by as much as 7% over networks accessed on foot. Bike sharing turned out to be the lowest-cost feeder option for the lion's share of cases studied. The walk-only feeder option won-out only in large-sized cities with high travel demands that were served by ordinary buses or BRT, even though the pre-existing transit networks were designed to suit access and egress on foot. The feeder-bus option never attained the lowest cost among the cases examined.

Not surprisingly, greater benefits could be achieved by optimizing trunk and feeder systems jointly. In these cases, shared bikes continued to be the lowest-cost feeder option for ordinary bus systems, and for BRT systems, in small-sized or low-demand cities. Feeder buses were winners in large-sized or high-demand cities with metro-rail systems. It bears noting that shared-bike feeder service might still be preferable in these latter cases, as it often imposed lower costs to the transit agency than did feeder buses. Savings in transit-agency cost could be used to subsidize shared-bike systems. In practice, subsidies could be achieved by discounting transit fares to shared-bike riders.

The numerical results presented in this chapter are limited, partly due to the large number of parameters in our models. Still, we believe that the experiments are sufficient to show that accessing transit via shared bikes is often worth considering. For a specific city, the applicable scope and benefits of a transit network fed by shared bikes can be derived from our model, should key parameter values (e.g., the intermodal transfer penalty t_f) of that city be available.

Of further note, the present findings came by means of simplified models for idealized cases. In some instances, the simplifications are conservative; e.g. recall that some short-distance commuters might enjoy greater cost savings by using shared bikes to cover their entire trips. This might justify trunk designs with larger line and station spacings (to serve longer-distance trips). The benefits might trigger favorable modal shifts, which could benefit transit, and was likewise not considered in the present study. New models are presently being developed to explore optimal system designs under more realistic operating scenarios that

account for mode choice and spatially heterogeneous demand. Consideration of demand heterogeneity may entail the use of continuum approximation techniques (e.g. Chien and Schonfeld, 1997; Ouyang et al., 2014). In addition, our modeling framework can be tuned to analyze transit systems fed by other access modes, e.g., scooters, e-bikes, and autonomous cars. Work in this regard is also underway.

Chapter 3

Improving bus priority and car discharge capacity at signalized intersections

3.1 Introduction and literature review

Buses and cars are the two major traffic modes that interact and compete for the road space in urban networks. The competition is especially intensive at roadway bottlenecks, including signalized intersections. Signalized intersections are common bottlenecks in urban traffic networks, which typically lead to large delays and restricted vehicular discharging capacities. Worse still, car discharging capacities at busy signalized intersections are further undermined due to the implementation of bus priority strategies, including transit signal priority (TSP) strategies and dedicated bus lanes (DBLs).

TSP can provide signal timing benefits to buses that cross an intersection (Lin et al., 2015). Commonly used schemes are active TSP schemes, which dynamically assign green times to ensure buses' early passes of the intersection (Garrow and Machemehl, 1997; Urbanik and Holder, 1977). Typical schemes include green extension (to facilitate buses arriving soon after the end of a green phase), red truncation (to facilitate buses arriving shortly before the end of a red phase), green insertion (to facilitate buses arriving in the middle of a red phase), etc., and their combinations. To ensure TSP schemes' operational efficiency, they were often jointly implemented with a DBL so that bus arrivals at the intersection are not impeded by downstream cars (Tan et al., 2006; Truong et al., 2017). However, a DBL alone can significantly diminish cars' discharging capacity and create long car queues (Zhou and Gan, 2005). Combination of TSP and DBL only makes the car traffic suffer more (Daganzo, 2007; Muthuswamy et al., 2007). As a result, bus priority strategies are considered unsuitable for busy intersections with heavy car traffic.

To ensure bus priority strategies are more widely accepted and applied, researchers have studied on means to alleviate damages made to cars by those priority strategies. A common strategy is termed the "intermittent bus lane" (IBL), which allows cars to use the bus lane when no bus is approaching (Eichler and Daganzo, 2006; Guler and Cassidy, 2012; Viegas

and Lu, 2001, 2004; Wu and Hounsell, 1998). IBL is often implemented with the assistance of a mid-block pre-signal installed a certain distance upstream of the intersection. A pre-signal cycle has two phases, red and green. During a red phase, cars are not allowed to pass the pre-signal and enter the downstream IBL. A red phase is activated a certain period prior to the predicted arrival time of an approaching bus, so that cars queueing in the IBL can be cleared before the bus enters the IBL. The bus can thus approach to the intersection without delay (or sometimes with a smaller delay if downstream cars are not fully dissipated). The pre-signal's green phase resumes after the bus passes the pre-signal. This strategy can reduce the cars' discharging capacity loss at the intersection while still ensuring buses are prioritized (Guler and Cassidy, 2012; Guler and Menendez, 2014a, 2014b; He et al., 2016; Wu and Hounsell, 1998). IBL can be further combined with TSP at the intersection.

IBLs can reduce the car discharging capacity loss created by bus priority, but only to a limited extent. This is because the clearance of car queues in an IBL prior to a predicted bus arrival creates "voids" in the lane where neither cars nor buses can use. The capacity loss due to these voids grows as the bus frequency increases (Qiu et al., 2015). Thus, we also seek other methods in the literature to further increase cars' discharging capacity. One innovative method proposed by Xuan et al. (2011) uses a mid-block pre-signal to sort conflicting traffic streams (e.g., left-turning and through-moving vehicles) in the same approach, so that each stream can use more lanes to discharge into the intersection during their respective green phases.

We use a 2-lane intersection approach as example to illustrate Xuan et al.'s design; see Fig. 3.1. Left-turning (L-) and through-moving (T-) vehicles queue up in separate lanes upstream of the pre-signal. The pre-signal alternately admits L- and T-vehicles into the lane area between the pre-signal and the intersection, which is termed the "sorting area". The two types of vehicle queues stack in tandem in the sorting area. Each queue will use both lanes to discharge during a separate phase of the signal at the intersection, which is termed the main signal in this chapter. In real designs, the number of lanes in the sorting area, and the numbers of L- and T-lanes upstream of the pre-signal can take arbitrary integer values. This tandem design only involves limited change of layout in one intersection approach, and its resulting capacity gain is relatively large (over 20% as reported by Xuan et al., 2011). Its benefit has also been verified by real-world applications (e.g., Luo, 2011). Moreover, the pre-signal used to sort car traffic can also be used to enforce IBL operations in the same intersection approach.

This means we can potentially combine IBL and the tandem-sorting pre-signal, as well as TSP, to promote both car and bus traffic.

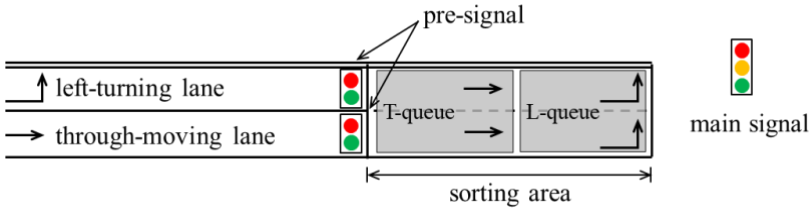

Fig. 3.1. Car lanes controlled by a pre-signal.

Literature is scarce on such an integrated design. Gu et al. (2015) proposed a design that combines TSP, DBL, and tandem-sorting pre-signal. The pre-signal's timing plan is adaptively coordinated with the main signal to provide bus signal priority. Analytical models for estimating expected bus delay and car discharge capacity, as well as the required sorting area length, were formulated. Numerical results showed that the new design could significantly reduce bus delays while still achieving some car capacity gains, as compared to the conventional case where neither pre-signal nor bus priority measure was included. The results indicated that TSP and bus lanes could be deployed at busy intersections where both car and bus flows are high, which was believed to be unprofitable by conventional wisdom. However, the above cited work is limited since only a simple TSP scheme, green extension, was modeled. The potential for further improving car traffic via IBL was also overlooked. A recent study (Bie et al., 2020) also examined selected instances of this design via simulation. However, this latter-cited work failed to unveil how key operating factors affect the performance metrics (i.e., bus and car delays and discharge capacities).

This study is an extension of Gu et al. (2015). We propose an integrated design that combines TSP schemes, pre-signal and the idea of IBL. The pre-signal is used not only to sort L- and T-traffic to improve the car discharge capacities, but also to control the entry of cars into the shoulder lane, so that approaching buses are prioritized. Four signal priority schemes are investigated: the first three are conventional ones including green extension, red truncation, and green insertion schemes, and the last one truncates the pre-signal's green phases only to clear the car queues in the shoulder lane before bus arrival. We term this last scheme "pre-signal green truncation" An algorithm is then proposed to select the most efficient scheme for each signal cycle, depending upon the real-time information (e.g., predicted bus arrival times).

Coordination between the pre-signal and main signal phases is presented to facilitate each signal priority scheme. Analytical models for estimating the two performance metrics, expected bus delay and car discharge capacity, are again formulated. Due to the greater complexity of mathematical models, we develop the results using numerical schemes instead of deriving closed-form formulas. Trade-off between these two conflicting metrics is examined by plotting the Pareto frontiers of the metrics. Results are compared against benchmark scenarios, including: (i) a design involving a DBL instead of the intermittent design; (ii) a design involving only the pre-signal for tandem sorting of L- and T-traffic streams, but neither TSP nor bus lane; and (iii) a conventional design where buses and cars are mixed, with no pre-signal, bus lane, or TSP. The comparison speaks to the value of introducing our proposed design, and more importantly, of optimally choosing the most efficient TSP scheme in real time.

The remainder of this chapter is organized as follows. Details of the proposed design are illustrated in Section 3.2. Models to determine the lane assignment, signal timing, expected bus delay and car discharge capacity under each TSP scheme are furnished in Section 3.3. Section 3.4 presents and compares numerical results, including Pareto frontiers between the two conflicting metrics, under all the scenarios for a variety of operating factors. Discussions and conclusions are presented in Section 3.5.

3.2 Proposed design

We first present the modeling framework in Section 3.2.1. The operating details for the pre-signal and the TSP schemes are described in Sections 3.2.2 and 3.2.3, respectively. A list of the notations used in this chapter is presented in Appendix A.

3.2.1 Modeling framework

We consider an approach to a four-way signalized intersection with at least three lanes, as illustrated in Fig. 3.2a. A pre-signal is placed a certain distance upstream of the intersection in all lanes sans the shoulder bus-lane. Arriving vehicles are assumed to be well-segregated upstream of the pre-signal: buses travel in the dedicated shoulder bus-lane, L-cars travel in the

left lane, and T-cars travel in the middle lane.[8] For simplicity, we assume all buses are through-moving. The L-cars and T-cars are rearranged in a tandem fashion in the sorting area as per Xuan et al. (2011). For the example shown in Fig. 3.2a, we assume L-cars can use the left and median lanes in the sorting area, while T-cars can use all three lanes in the sorting area to discharge.

Fig. 3.2b shows the order of phases of the main signal, where G_L and G_T are the green phases dedicated for L- and T-vehicles on the approach in consideration, respectively; and R_L and R_T are the green phases for the cross-street traffic[9]. An amber duration of $t_y = 3$ s is inserted between any two consecutive phases. The cycle length is denoted by $T = G_L + G_T + R_L + R_T + 4t_y$. This phase order is selected to shorten the vehicle queue lengths in the sorting area according to the *phase swap sorting strategy* from Xuan (2011). Note that long sorting areas may be inflexible to implement in short city blocks. Phase durations are optimized using a model presented in Section 3.3.

We further assume that car arrivals in each car-lane are deterministic with a uniform rate, and that bus arrivals follow a Poisson process with a constant rate λ_b. We then employ the kinematic wave theory (Lighthill and Whitham, 1955; Richards, 1956) to model the vehicle traffic in the sorting area. To this end, we assume that the vehicle traffic states occurring in a lane follow a triangular fundamental diagram, and traffic states occurring in a road segment of $n > 1$ lanes follow the lane-based fundamental diagram scaled by n. Fig. 3.2c depicts the fundamental diagrams of traffic in the 3-lane sorting area (see Fig. 3.2a) in moving-time coordinates (Newell, 1993). With a moving-time coordinate, slopes (representing speeds) in these fundamental diagrams are tilted toward left, such that the free-flow speed is represented by vertical lines (i.e., with infinite slope). Car traffic states that may arise in the sorting area are marked on the fundamental diagrams, including: saturated flow states S_i, jam states J_i, and discharge flows from the pre-signal, A_i, where $i = L$ for L-traffic, and $i = T$ for T-traffic. Denote q_S the saturation flow per travel lane, and N_L, N_T the numbers of lanes used by L- and T-traffic in the sorting area, respectively, then the saturation flow of state S_i, denoted Q_i, is

[8] If the approach has more than three lanes, the number of L- or T-lanes can be greater than 1.

[9] Right-turning cars may use a curbside bus lane temporarily to discharge without disturbing buses (The City of New York Government, 2018). Thus, we assume the right-turning traffic is small, and is combined with the T-traffic for analysis.

given by $Q_i = N_i q_S$, $i \in \{L, T\}$. Further denote n_L and n_T as the numbers of L- and T-lanes upstream of the pre-signal, respectively, then the flow of state A_i, denoted q_i, is given by $q_i = n_i q_S$, $i \in \{L, T\}$.[10] The w, w_L and w_T in Fig. 3.2c are speeds of shockwaves between corresponding traffic states. The w is given by the lane-based fundamental diagram, and w_L, w_T are given by the kinematic wave theory as: $w_L = \frac{n_L}{N_L} w$, $w_T = \frac{n_T}{N_T} w$.

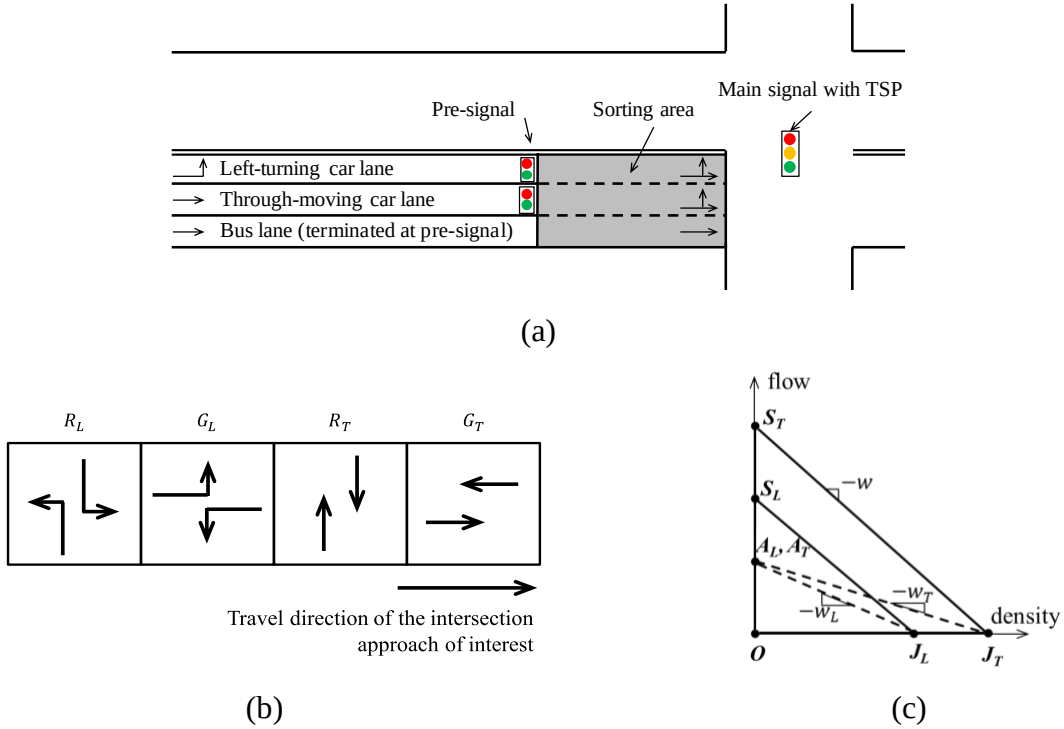

Fig. 3.2. A 3-lane intersection approach with integrated design: (a) the geometric layout; (b) the phase order of main signal; (c) fundamental diagrams in moving-time coordinate.

The fundamental diagrams will be built upon to plot time-space diagrams describing vehicle traffic states in the approach. These time-space diagrams will be used in the following sections to explain pre-signal and TSP operations under various conditions.

3.2.2 Pre-signal operations

A pre-signal cycle consists of no more than four phases: green phases for L- and T-vehicles, g_L and g_T, respectively, and red phases in between (if needed). An amber time of t_y is inserted

[10] For the example in Fig. 3.2, $n_L = n_T = 1$, $N_L = 2$, and $N_T = 3$.

between any two consecutive phases. Hence, we have: $g_L + g_T + 2t_y \leq T$. The pre-signal green phases are timed to ensure that any vehicle entering the sorting area can discharge into the intersection through a corresponding main-signal green phase. This means, first, that the duration of each pre-signal green phase is capped by the discharging capacity of the corresponding main-signal phase; and second, that a pre-signal green phase ends at least $\frac{d}{v_f}$ earlier than the end of the corresponding main-signal phase, where d is the length of sorting area, and v_f denotes vehicles' free-flow speed[11]. The first condition means $g_L n_L \leq G_L N_L$ and $g_T n_T \leq G_T N_T - \frac{\lambda_b T \delta}{q_S}$, where δ denotes the passenger car equivalent of a bus, which takes the value of 3.5 (Ahuja et al., 2003), and $\frac{\lambda_b T \delta}{q_S}$ is the average green time used to discharge T-buses in the shoulder lane in each cycle.[12] The second condition allows the last vehicle passing the pre-signal in a green phase to discharge into the intersection without being delayed till the next cycle. This pre-signal timing plan is coordinated with the main signal in a similar fashion to Xuan et al. (2011) to maximize car discharge capacity, and will be adjusted dynamically in response to any TSP changes at the main signal. The g_L and g_T, together with n_L and n_T, are again optimized using a model furnished in Section 3.3.

To help readers better understand the vehicle operations regulated by the pre-signal, we note that three cases of queueing patterns may arise in the sorting area. In case (i), L- and T-queues formed in the sorting area are temporally separated. This case occurs when $g_L \leq G_L + R_L + t_y$ and $g_T \leq G_T + R_T + t_y$ both hold. This is illustrated by the time-space diagram in Fig. 3, where J_L and J_T represent L- and T-queues, respectively, and O represents the state with no traffic. Fig. 3.3 is also plotted with the moving-time coordinate, such that vertical lines in the

[11] For simplicity, in this chapter we assume buses and cars have the same free-flow speed. In reality, a bus cruising slower than cars becomes a moving bottleneck for upstream cars. Considering this moving-bottleneck effect will complicate the analysis, but our modelling approach can still be applied to this more realistic scenario.

[12] The actual number of bus arrivals in a cycle is a random variable, meaning that the upper bound of g_T varies across cycles. Thus, condition $g_T n_T \leq G_T N_T - \frac{\lambda_b T \delta}{q_S}$ should be interpreted on an average basis. However, this does not affect the calculation of performance metrics in Section 3.3, i.e., the expected bus delay and car discharge capacity. In practice, the pre-signal phases can be controlled by detectors installed on approaching lanes. Each detector counts the number of equivalent cars passing the pre-signal (with one bus counted as δ cars) and terminates the corresponding green phase when the number hits a threshold.

figure represent vehicles or traffic state interfaces traveling at the free-flow speed.[13] Case (ii) occurs when $g_L > G_L + R_L + t_y$. In this case a L-queue will be stacked on top (upstream) of a T-queue in the left and median lanes. Similarly, case (iii) arises when $g_T > G_T + R_T + t_y$. In this last case a T-queue will be stacked on top of a L-queue in the two left-most lanes. Illustrations of the latter two cases are omitted for simplicity. (Note that $g_L > G_L + R_L + t_y$ and $g_T > G_T + R_T + t_y$ cannot be simultaneously satisfied, since $g_L + g_T + 2t_y \leq T = G_L + G_T + R_L + R_T + 4t_y$.)

Note that the pre-signal does not control approaching buses, which can always enter the sorting area without delay. If a bus crosses the pre-signal before the start of g_T phase in a cycle, it would proceed all the way to the stop line of intersection since L-cars do not queue up in the shoulder lane. The bus would thus be the first one to discharge in the next G_T phase. On the other hand, a bus entering the sorting area during a g_T phase may join the T-queue formed in the shoulder lane, should no TSP scheme be activated. In this latter case the bus may experience some delay.

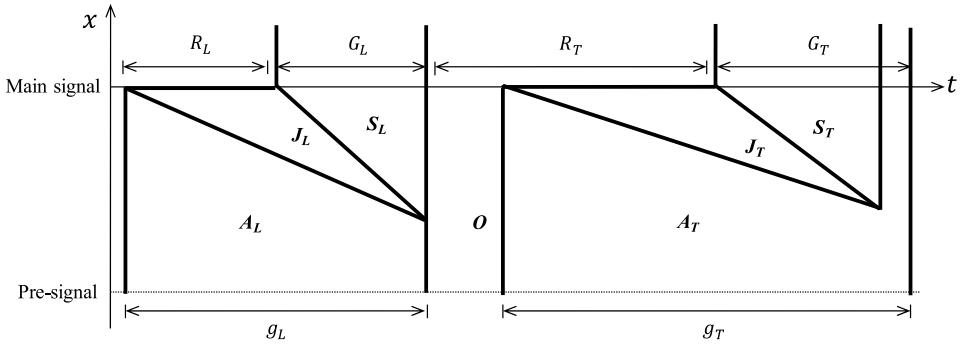

Fig. 3.3. Separated L- and T-queues.

[13] Caveats: (i) the offset between the ends of a pre-signal green phase and the corresponding main signal phase, d/v_f, cannot be seen under the moving-time coordinate; and (ii) the figure is not a rigorous time-space diagram since L-vehicles only occupy the left and median lanes, while T-vehicles occupy all the three lanes. However, no ambiguity arises here since the two queues are fully separated.

3.2.3 TSP schemes

The first three TSP schemes, i.e., green extension, red truncation, and green insertion, will grant green times in a timely manner to through-moving buses (and T-cars sometimes). To be conservative and convenient for the modeling work, we devise these schemes in a way that minimizes the negative impacts on other traffic streams and on following cycles. Specifically, we stipulate that the green times allocated to other traffic streams (i.e., G_L, R_T, and R_L) are not shortened. They will be either postponed (in the case of green extension), or suspended but resumed later. The duration of green extension or insertion will be deducted from the next G_T phase. By doing so, discharge capacities of other traffic streams are not compromised.[14] Moreover, changes incurred by an approaching bus will only affect the present cycle in which the bus arrives, not any following cycles. (The above are also true for pre-signal green truncation since it does not alter phases of the main signal.) This allows us to build models based upon a single generic cycle. Note too that under these schemes, only T-cars may suffer discharge capacity losses. This also renders the performance on car traffic easy to assess. For the convenience of practical implementation, we assume that no more than one TSP scheme is applied in each signal cycle. Further assume that bus arrival times to the pre-signal and the intersection can be accurately predicted. Details for each TSP scheme are explained in the following sections.

3.2.3.1 Green extension

Green extension applies to buses that are predicted to arrive at the intersection shortly after the end of a G_T phase. Those buses would otherwise experience long delays before they are served by the next G_T. We define $G_{T0} \leq G_T$ as green extension duration, so that if a bus is predicted to arrive t_a after the end of G_T and $t_a \leq G_{T0}$, the bus will cross the intersection without delay; see Fig. 3.4. The figure shows the original signal phases and a bus trajectory in moving-time coordinate in the upper part, and the signal phases under green extension and the modified trajectory of the same bus in the lower part. We set the end time of last G_T to zero. The following R_L, G_L, and R_T phases are postponed by G_{T0}, and the next G_T is reduced by G_{T0} to

[14] However, vehicles in other streams may experience delays due to the postponed green phases.

ensure the cycle length remains unchanged. The bus delay saving can be seen by comparing the discharging bus trajectories in the upper and lower parts of the figure.

The pre-signal green phase g_T does not need be truncated like G_T if the truncated main-signal phase $G_T - G_{T0}$ is still sufficient to discharge all T-cars and buses that pass through g_T. This means $G_{T0} \leq G_T - \frac{\lambda_b T\delta}{N_T q_S} - \frac{g_T n_T}{N_T}$, where the RHS means the redundant green time in a G_T phase. In this case, green extension does not reduce the T-car capacity. If, on the other hand, $G_{T0} > G_T - \frac{\lambda_b T\delta}{N_T q_S} - \frac{g_T n_T}{N_T}$, then g_T must be shortened to $g'_T = \frac{N_T}{n_T}\left(G_T - \frac{\lambda_b T\delta}{N_T q_S} - G_{T0}\right)$, so that all T-cars entering the sorting area can fully discharge into the intersection during the trimmed green phase. In short, the new pre-signal green phase is $g'_T = \min\left\{g_T, \frac{N_T}{n_T}\left(G_T - \frac{\lambda_b T\delta}{N_T q_S} - G_{T0}\right)\right\}$[15].

Parameter G_{T0} is a proxy of the degree of bus priority. A larger G_{T0} renders more bus delay savings, but also a greater T-car capacity loss.

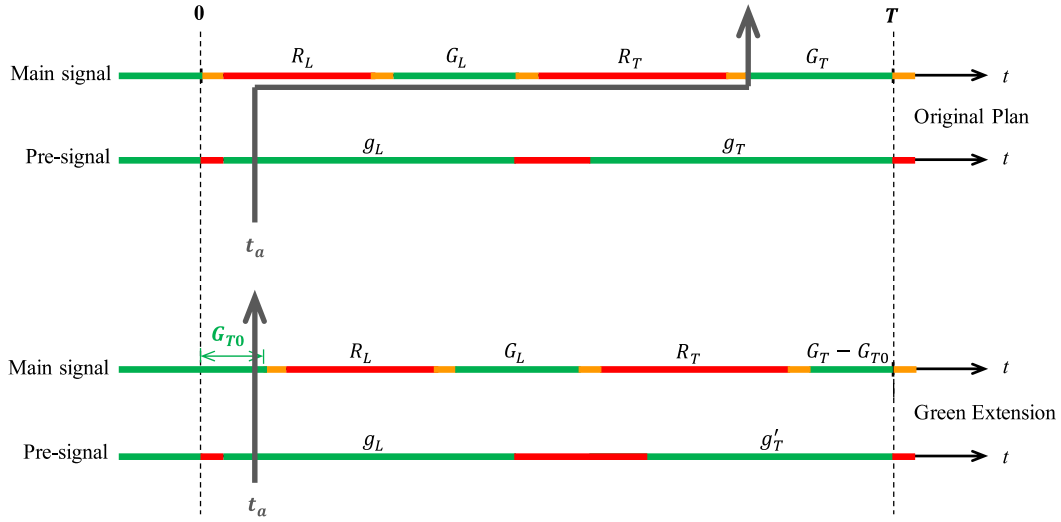

Fig. 3.4. Illustration of green extension.

[15] Again, this should be interpreted on an average basis. In practice, one can terminate the pre-signal green phase when $q_S g'_T n_T + \lambda_b T\delta$ equivalent cars are counted. This control is conservative since under TSP schemes some buses do not discharge during a regular G_T phase. The same method can also be applied to red truncation and green insertion to be described next.

3.2.3.2 Red truncation (early green)

Red truncation applies to buses that arrive to the intersection earlier than the start of a G_T phase. Thus, bus delay savings created by red truncation are relatively small as compared to green extension. This scheme is illustrated in Fig. 3.5, where the predicted bus arrival time at intersection, again denoted t_a, occurs in the R_T phase. The red phase is truncated to duration $R'_T \in [0, R_T - t_y]$, followed by an advanced green phase of duration $G_T - t_y$. The bus then discharges together with T-cars during this advanced green phase. It is reduced from G_T to $G_T - t_y$ because red truncation will create an additional amber phase. The red phase then resumes after that green phase and lasts until the end of cycle. The duration of resumed red phase is $R_T - R'_T$.

To ensure T-cars entering the sorting area can discharge in time, the g_T phase is shortened to $g'_T = \min\left\{g_T, g_T - R_T + R'_T - t_y + \max\{0, g_L - (R_L + G_L + t_y)\}, \frac{N_T}{n_T}\left(G_T - \frac{\lambda_b T \delta}{N_T q_S} - t_y\right)\right\}$. The second term in the braces represents the case where g_T is truncated from the right end echoing the change of G_T's right end. The last term in the braces represents the case where the reduced phase of $G_T - t_y$ will be saturated if the maximum number of T-cars pass through the pre-signal. Note that red truncation cannot fully eliminate delay of a prioritized bus (e.g., the one shown in Fig. 3.5), since the bus may join a T-queue in the sorting area before discharging into the intersection.

The scheme essentially advances the original G_T phase by $R_T - R'_T$ (and reduces it by t_y). All bus arrivals during the advanced green phase will be prioritized. On the other hand, buses that arrive in the original G_T but miss the advanced green phase will have to wait till the next G_T to discharge. Those buses will experience greater delays. Thus, the overall performance of the red truncation scheme depends on the predicted bus arrival times and the choice of parameter R'_T.

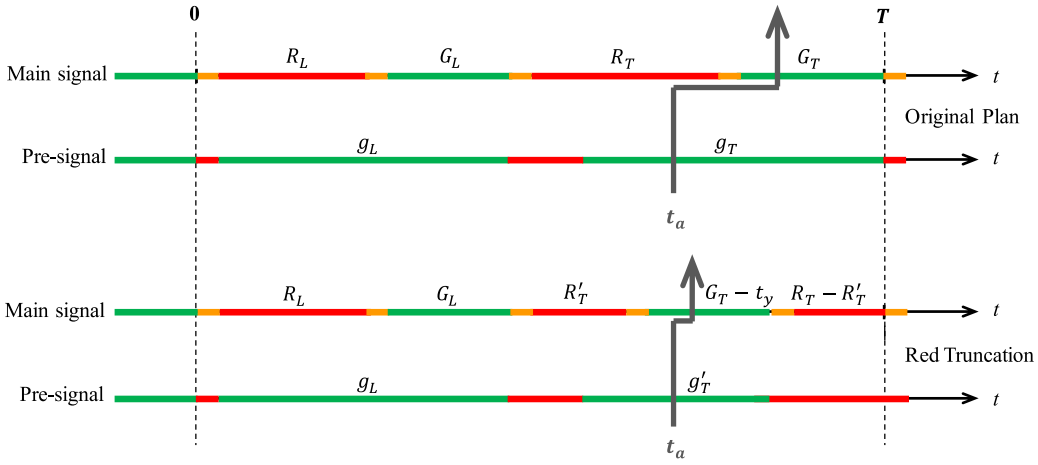

Fig. 3.5. Illustration of red truncation.

3.2.3.3 Green insertion

Green insertion is more flexible and can practically be used to prioritize buses arriving at any time of a cycle. Nevertheless, for simplicity we assume in this chapter that green insertion only applies to predicted bus arrivals in a G_L or R_T phase, while those arrivals in R_L phases will be handled by green extension. Under this scheme, a short green phase of duration G_B is inserted in the middle of a G_L or R_T to entertain approaching buses. The interrupted phase resumes after the inserted G_B. We denote the two phases separated by G_B as G_{L1} and $G_{L2} = G_L - G_{L1}$ for an insertion into G_L, and as R_{T1} and $R_{T2} = R_T - R_{T1}$ for an insertion into R_T; see the two cases illustrated in Fig. 3.6a and b, respectively. In each case, a green insertion is defined by two parameters: its start time, specified by G_{L1} or R_{T1}, and its duration $G_B \in \left[\frac{\delta}{q_S}, G_T - 2t_y\right]$. Since the insertion includes two amber phases, the next G_T will be reduced to $G_T - G_B - 2t_y$.[16] The g_T phase will be truncated from the left echoing the reduced G_T. The truncated phase duration is $g'_T = \min\left\{g_T, \frac{N_T}{n_T}\left(G_T - \frac{\lambda_b T \delta}{N_T q_S} - G_B - 2t_y\right)\right\}$. This is conservative because some T-cars

[16] Under circumstances where a G_B is inserted next to an existing amber phase, only one more amber phase will be inserted. However, we ignore this trivial case for simplicity and conservativeness.

passing the pre-signal may discharge into the intersection during G_B. We time the pre-signal in this conservative way for the modeling simplicity.

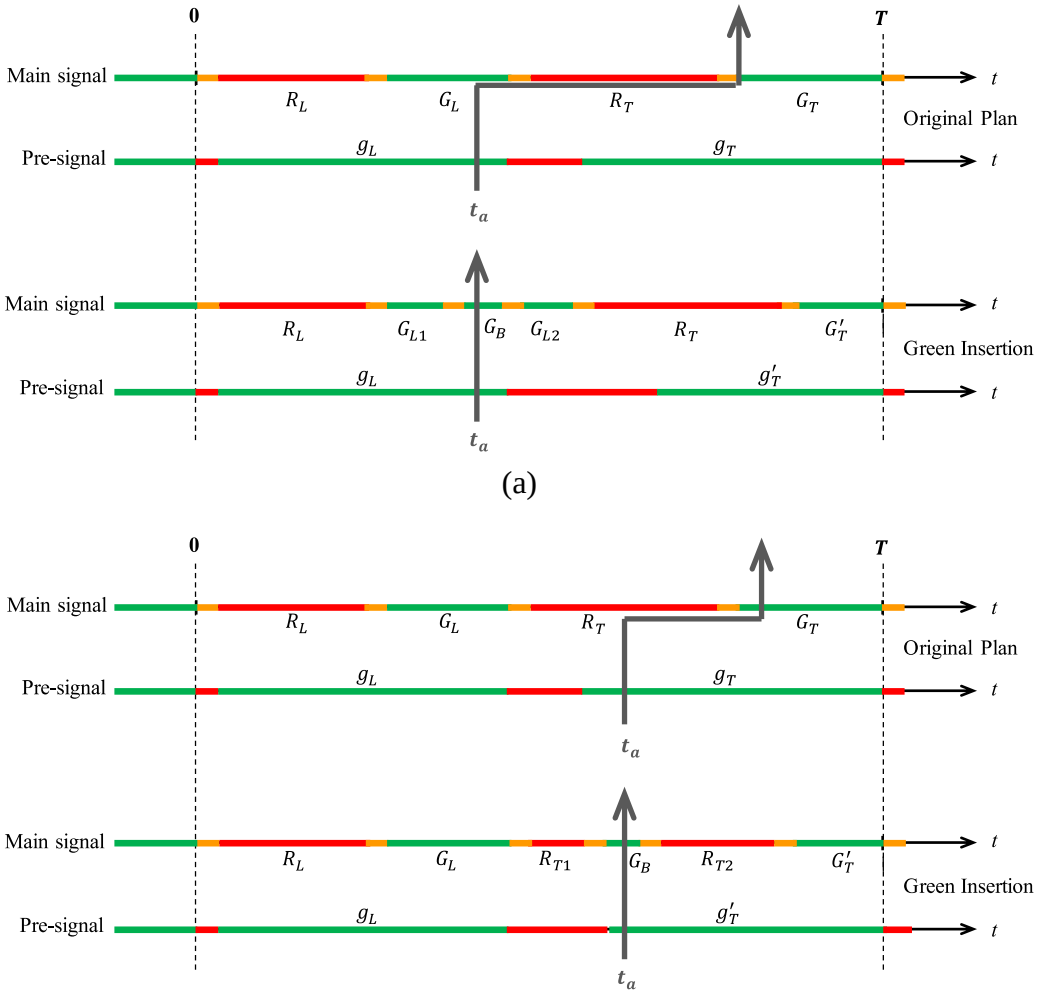

Fig. 3.6. Illustration of green insertion: (a) insertion into a G_L phase; (b) insertion into a R_T phase.

3.2.3.4 Pre-signal green truncation

This scheme applies to bus arrivals at the pre-signal during a g_T phase. It alters the pre-signal phases only, but not the main signal phases. The scheme is illustrated in Fig. 3.7, where the g_T phase starts as normal, but is truncated at duration g_{T1}. T-cars entering the sorting area during g_{T1} are discharged during the first part of G_T, and the pre-signal green phase resumes next. Thus, the resumed duration is $g_{T2} = G_T - \frac{\lambda_b T \delta}{N_T q_S} - \frac{g_{T1} n_T}{N_T}$, and the total pre-signal green duration

is $g'_T = g_{T1} + g_{T2}$. Buses arriving from the start of g_{T1} to the start of g_{T2} will experience shorter delays, and those arriving during g_{T2} will experience no delay.

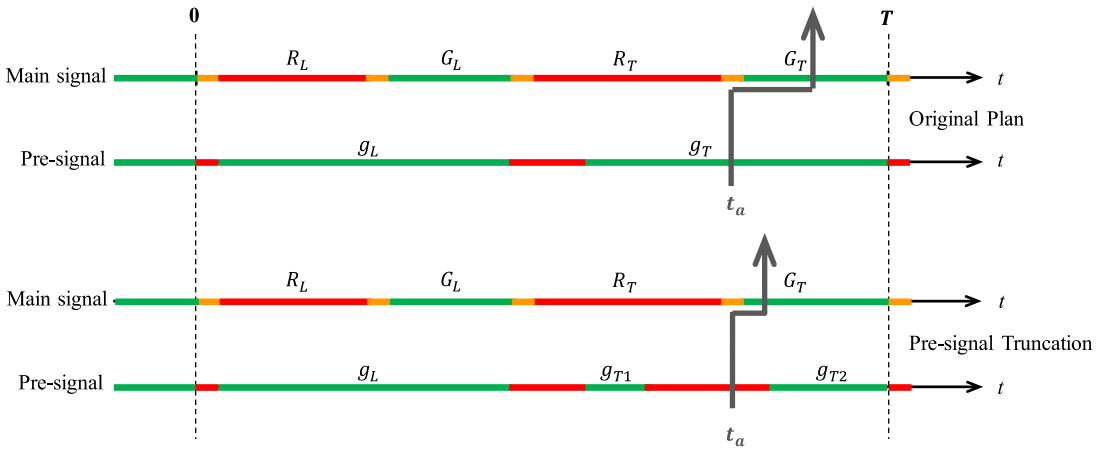

Fig. 3.7. Illustration of pre-signal green truncation.

3.2.3.5 A dynamic TSP scheme

Each of the four schemes discussed above has one or two parameters (i.e., G_{T0} for green extension, R'_T for red truncation, G_{L1}, R_{T1} and G_B for green insertion, and g_{T1} for pre-signal green truncation), which can be selected optimally to minimize an objective (e.g., a weighted sum of bus delay saving and car discharge capacity). However, each scheme suits only a subset of bus arrivals and has its own limitations. Thus, we propose a dynamic scheme that selects the best among the four for each signal cycle, based upon a common objective. The optimization models and a solution method are presented next.

3.3 Models and solution method

The objective function, together with the car capacity and total bus delay in a cycle, are formulated in Section 3.3.1. The optimal plans of main and pre-signal and the lane assignment are modeled in Section 3.3.2, assuming no TSP alteration is activated. Section 3.3.3 furnishes models for estimating bus delays under each of the four TSP schemes, respectively. A solution method is provided in Section 3.3.4.

3.3.1 Objective function

The objective function is expressed as a weighted sum of T-cars' discharge capacity and negative total bus delay in an arbitrary cycle. We choose the T-car capacity only because TSP only undermines the capacity of T-cars but not the L-cars. Specifically,

$$W = \max\{(1-r)Q_T + r \cdot (-D_B)\}, \tag{3.1}$$

where $r \in [0,1]$ is the weight for the bus delay term; Q_T the maximum number of T-cars that can discharged in a cycle; and D_B the total bus delay in the same cycle. The Q_T and D_B are given as follows:

$$Q_T = Q(N,n) \cdot (1-l)T\frac{g_T'}{g_T}, \tag{3.2}$$

$$D_B = \sum_{a=1}^{m} d_b(t_a), \tag{3.3}$$

where $Q(N,n)$ denotes the maximum vehicle discharge capacity in the absence of TSP, for an approach with N lanes in the sorting area and n lanes for L- and T-cars upstream of the pre-signal (for the case shown in Fig. 3.2a, $N = 3$ and $n = 2$); l denotes the left-turning ratio of the subject approach; m denotes the number of bus arrivals in the cycle; and $d_b(t_a)$ is the delay for the a-th arriving bus, which is predicted to arrive to the intersection at $t_a \in (0,T]$. Objective (3.1) is maximized for each signal cycle separately. The optimal decision pertains to whether a TSP scheme and which scheme should be called, and the optimal parameter value(s) for the scheme selected.

The $Q(N,n)$ is developed using the model furnished next.

3.3.2 Optimal signal timing and lane assignment

We borrow the integer program from Xuan et al. (2011), with moderate modifications, to optimize the main and pre-signal phases and lane assignment. The following parameters are given before the optimization: the total green time assigned to the subject approach, $G = G_L + G_T$; the left-turning ratio l; and the number of car-lanes upstream of pre-signal, n; and the numbers of L- and T-lanes in the sorting area, $N_L = N - 1$, $N_T = N$, respectively. The modified integer program is given as follows:

$$Q(N,n) = \max_{n_L,n_T}\left\{q = q_s \cdot \min\left\{\frac{\frac{G}{T}-\frac{\lambda_b\delta}{N_T q_S}}{lN_L^{-1}+(1-l)N_T^{-1}}, \frac{1-2t_y T^{-1}}{ln_L^{-1}+(1-l)n_T^{-1}}\right\}\right\} \quad (3.4a)$$

subject to:

$$n_L + n_T = n \quad (3.4b)$$

$n_L, n_T \geq 1$, and are integers (3.4c)

where $Q(N,n)$ denotes the maximum car discharge capacity (combining both L- and T-cars) of an intersection with N lanes in the sorting area ($N-1$ lanes are used by L-cars; see Fig. 3.2a), and n car-lanes upstream of the pre-signal. This program can be easily solved by exhaustive search.

After obtaining the optimal n_L and n_T, the optimal green phase durations of the main and pre-signals are derived as follows:

$$g_T = \frac{T(1-l)}{q_s n_T} \cdot Q(N,n) \quad (3.5a)$$

$$g_L = \frac{Tl}{q_s n_L} \cdot Q(N,n) \quad (3.5b)$$

$$G_L = \frac{g_L n_L}{N_L} \quad (3.5c)$$

$$G_T = G - G_L \quad (3.5d)$$

where (3.5d) allocates the redundant green time at the main signal (if any) to the G_T phase, so that the car capacity loss caused by TSP can be partially compensated.

3.3.3 Bus delay models

We first develop the bus delay model for a benchmark cycle where no TSP scheme is activated in Section 3.3.3.1. Models under each of the four TSP schemes are presented in Sections 3.3.3.2-3.3.3.5, respectively.

3.3.3.1 Bus delay in a benchmark cycle

We first define two time variables as illustrated in the time-space diagram in Fig. 3.8: T_1 and T_2 be the start of g_T and G_T phases, respectively, and T_3 be the time when the T-car queue fully dissipates, taking the start of cycle as time zero. They are calculated as follows:

$$T_1 = T - g_T - \max\{0, g_L - (R_L + G_L + t_y)\}$$

$$T_2 = T - G_T$$

$$T_3 = T_2 + \frac{(T_2 - T_1)\cdot n_T}{(N_T - n_T)}.$$

Note that Fig. 3.8 only illustrates the case where L- and T-queues in the sorting area are separated. However, the equations in this section are developed for all the three cases of queue formation as explained in Section 3.2.2. For example, the second term in max{} of the equation of T_1 applies when $g_L - (R_L + G_L + t_y) > 0$, which means a L-queue will queue upstream of a T-queue in the sorting area.

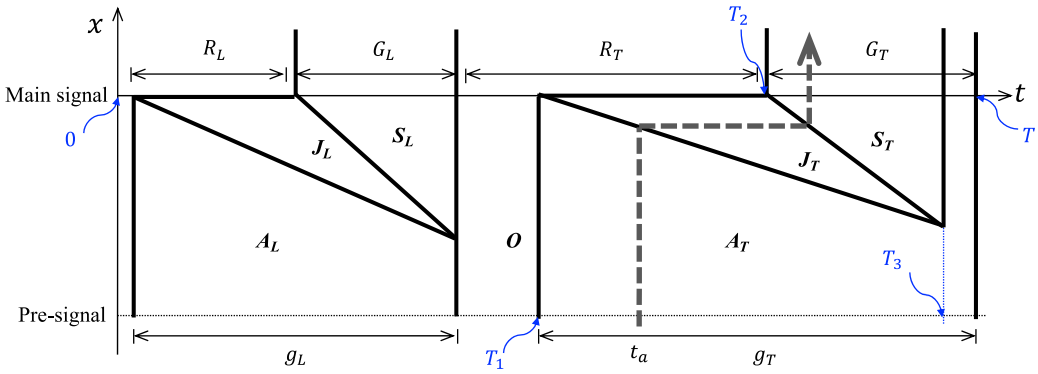

Fig. 3.8. Time-space diagram for a benchmark cycle.

The delay of a bus with arrival time $t_a \in (0, T]$ depends on which interval t_a falls in: if $t_a \in (0, T_1]$, the arriving bus will proceed to the stop line and be the first to discharge in G_T; if $t_a \in (T_1, T_3]$, the bus will queue up after some T-cars in the shoulder lane (see the dashed bus trajectory in Fig. 3.8); and if $t_a \in (T_3, T]$, the bus may experience no delay, or some delay if g_T is forced to shift leftward due to a too long g_L (see case (ii) in Section 3.2.2). By geometry, the bus delay is formulated as:

$$d_{b,0}(t_a) = \begin{cases} T_2 - t_a, & \text{if } t_a \in (0, T_1] \\ (T_3 - t_a)\frac{(N_T - n_T)}{N_T}, & \text{if } t_a \in (T_1, T_3] \\ \max\{0, T + T_3 - T_1 - g_T - t_a\} \cdot \frac{2T - G_T - t_a}{T - t_a}, & \text{if } t_a \in (T_3, T] \end{cases} \quad (3.6)$$

3.3.3.2 Bus delay under green extension

The delay of bus arriving at t_a under a green extension of G_{T0}, $d_{b,1}(t_a|G_{T0})$, is presented as follows:

$$d_{b,1}(t_a|G_{T0}) = \begin{cases} 0, & \text{if } t_a \in (0, G_{T0}] \\ T_2 - t_a, & \text{if } t_a \in (G_{T0}, T_1] \\ (T_3 - t_a)\frac{(N_T - n_T)}{N_T}, & \text{if } t_a \in (T_1, T_3] \\ \max\{0, T + T_3 - T_1 - g'_T - t_a\} \cdot \frac{2T - G_T - t_a}{T - t_a}, & \text{if } t_a \in (T_3, T] \end{cases} \quad (3.7)$$

where T_1 and T_2 are the start of g'_T and G'_T phases, respectively, and T_3 the time when the T-car queue fully dissipates (see Fig. 3.9). They are given by:

$$T_1 = T - g'_T - \max\{0, g_L - (R_L + G_L + t_y)\}$$

$$T_2 = T - G'_T$$

$$T_3 = T_2 + \frac{(T_2 - T_1) \cdot n_T}{(N_T - n_T)}$$

$$G'_T = G_T - G_{T0}$$

$$g'_T = \min\left\{g_T, \frac{N_T}{n_T}\left(G'_T - \frac{\lambda_b T \delta}{N_T q_S}\right)\right\}$$

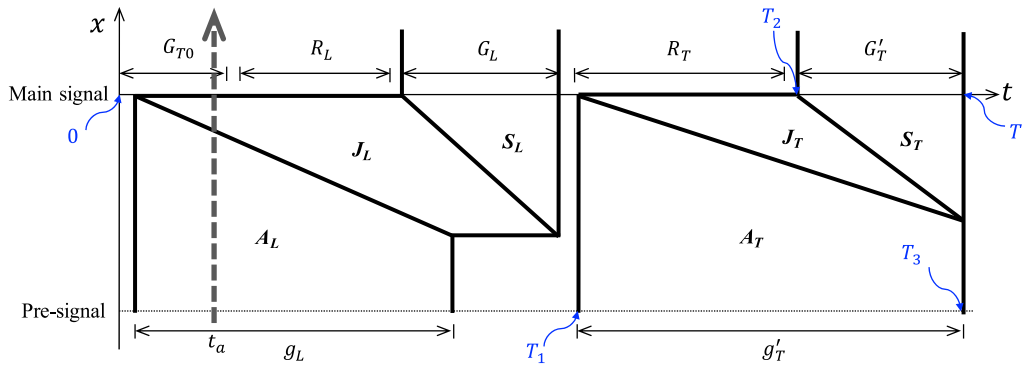

Fig. 3.9. Time-space diagram for a cycle with green extension.

3.3.3.3 Bus delay under red truncation

The delay of bus arriving at t_a under a red truncation at R'_T, $d_{b,2}(t_a|R'_T)$, is given as follows:

$$d_{b,2}(t_a|R'_T) = \begin{cases} T_2 - t_a, & \text{if } t_a \in (0, T_1] \\ (T_3 - t_a)\frac{(N_T - n_T)}{N_T}, & \text{if } t_a \in (T_1, T_3] \\ 0, & \text{if } t_a \in (T_3, T_4] \\ 2T - G_T - t_a, & \text{if } t_a \in (T_4, T] \end{cases} \tag{3.8}$$

where T_1, T_2, T_3 and T_4 (see Fig. 3.10) are given by:

$$T_1 = T - g'_T - \max\{0, g_L - (R_L + G_L + t_y)\}$$

$$T_2 = T - G_T - R_T + R'_T$$

$$T_3 = T_2 + \frac{(T_2 - T_1)\cdot n_T}{(N_T - n_T)}$$

$$T_4 = T - R_T + R'_T - t_y$$

$$G'_T = G_T - t_y$$

$$g'_T = \min\left\{g_T, g_T - R_T + R'_T - t_y + \max\{0, g_L - (R_L + G_L + t_y)\}, \frac{N_T}{n_T}\left(G'_T - \frac{\lambda_b T \delta}{N_T q_S}\right)\right\}$$

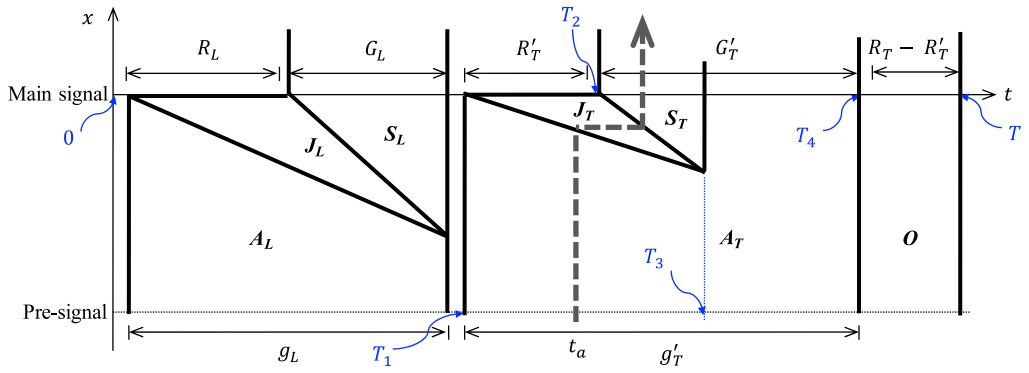

Fig. 3.10. Time-space diagram under red truncation.

3.3.3.4 Bus delay under green insertion

This is the most complicated case. To simplify, we consider two cases where a G_B starts earlier and later than g'_T, respectively. They are illustrated in Fig. 3.11a and b. The first case occurs when $T_1 < T_3$, where $T_1 = \begin{cases} R_L + G_{L1} + 3t_y, \text{for an insertion into } G_L \\ R_L + G_L + R_{T1} + 4t_y, \text{for an insertion to } R_T \end{cases}$, and $T_3 = T - g'_T - \max\{0, g_L - (R_L + G_L + t_y)\}$. In this case, G_B should serve an approaching bus before any T-car starts to enter the sorting area. Thus, this G_B should start right when a bus arrives at the intersection, and be short enough to only accommodate that bus, i.e., $G_B = \frac{\delta}{q_S}$. However, other buses' delays may also be affected by the green insertion. Thus, we derive the delay of bus arriving at t_a under this case, $d_{b,31}\left(t_a \middle| G_{L1}, R_{T1}, G_B = \frac{\delta}{q_S}\right)$ as the equation below. Note that we specify $G_{L1} \in [t_y, G_L - t_y]$ and $R_{T1} = T$ if the insertion is into G_L, and specify $G_{L1} = T$ and $R_{T1} \in [t_y, R_T - t_y]$ if the insertion is into R_T.

$$d_{b,31}\left(t_a \middle| G_{L1}, R_{T1}, G_B = \frac{\delta}{q_S}\right) = \begin{cases} T_1 - t_a, & \text{if } t_a \in (0, T_1] \\ 0, & \text{if } t_a \in (T_1, T_2] \\ T_4 - t_a, & \text{if } t_a \in (T_2, T_3] \\ (T_5 - t_a)\frac{(N_T - n_T)}{N_T}, & \text{if } t_a \in (T_3, T_5] \\ \max\{0, T + T_5 - T_3 - g'_T - t_a\} \cdot \frac{2T - G_T - t_a}{T - t_a}, & \text{if } t_a \in (T_5, T] \end{cases} \tag{3.9}$$

where T_2, T_4 and T_5 (see Fig. 3.11a) are given by:

$$T_2 = T_1 + G_B$$

$$T_4 = T - G'_T$$

$$T_5 = T_4 + \frac{(T_4 - T_3) \cdot n_T}{(N_T - n_T)}$$

$$G'_T = G_T - G_B - 2t_y$$

$$g'_T = \min\left\{g_T, \frac{N_T}{n_T}\left(G'_T - \frac{\lambda_b T \delta}{N_T q_S}\right)\right\}$$

The second case occurs when $T_1 \geq T_3$, where T_1 and T_3 were defined above. In this case, a bus arriving during G_B will join a T-queue in the shoulder lane, and the T-cars queued downstream of the bus will first discharge into the intersection during G_B before the bus does. The delay of bus arriving at t_a under this case, $d_{b,32}(t_a|G_{L1}, R_{T1}, G_B)$ is given below, for $G_B \in [t_y, G_T - 2t_y]$, $G_{L1} \in [t_y, G_L - t_y]$, and $R_{T1} \in [t_y, R_T - t_y]$. We again set $R_{T1} = T$ for an insertion into G_L, and $G_{L1} = T$ for an insertion into R_T.

$$d_{b,32}(t_a|G_{L1}, R_{T1}, G_B) = \begin{cases} T_1 - t_a, & \text{if } t_a \in (0, T_3] \\ (T_6 - t_a)\frac{(N_T - n_T)}{N_T}, & \text{if } t_a \in (T_3, T_6] \\ 0, & \text{if } t_a \in (T_6, T_2] \\ (T_5 - t_a)\frac{(N_T - n_T)}{N_T}, & \text{if } t_a \in (T_2, T_5] \\ \max\{0, T + T_5 - T_3 - g'_T - t_a\} \cdot \frac{2T - G_T - t_a}{T - t_a}, & \text{if } t_a \in (T_5, T] \end{cases} \quad (3.10)$$

where T_2 and T_4 are the same as in the first case, while T_5 (redefined) and T_6 (see Fig. 3.11b) are given by:

$$T_5 = T_4 + \frac{(T_4 - T_2) \cdot n_T}{(N_T - n_T)}$$

$$T_6 = T_1 + \frac{(T_1 - T_3) \cdot n_T}{(N_T - n_T)}$$

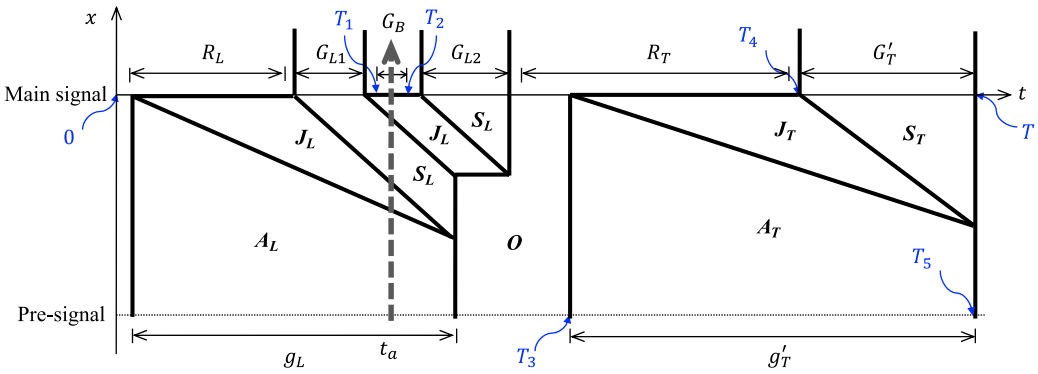

(a)

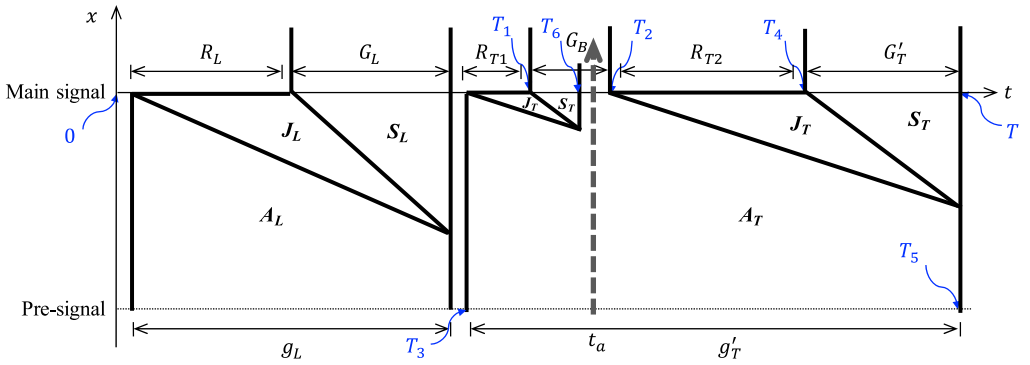

(b)

Fig. 3.11. Time-space diagrams under green insertion: (a) G_B starts earlier than g'_T; (b) G_B starts later than g'_T.

3.3.3.5 Bus delay under pre-signal green truncation

The delay of a bus arriving at t_a under a pre-signal green truncation with parameter g_{T1}, $d_{b,4}(t_a|g_{T1})$, for $g_{T1} \in \left[t_y, \left(g_T - G_T + max\{0, g_L - \left(R_L + G_L + t_y\right)\}\right)\right]$, is given by:

$$d_{b,4}(t_a|g_{T1}) = \begin{cases} T_3 - t_a, & \text{if } t_a \in (0, T_1] \\ (t_a - T_1)\frac{n_T}{N_T} + (T_3 - t_a), & \text{if } t_a \in (T_1, T_2] \\ T_4 - t_a & \text{if } t_a \in (T_2, T_4] \\ 0, & \text{if } t_a \in (T_4, T] \end{cases} \tag{3.11}$$

where T_1, T_2, T_3 and T_4 (see Fig. 3.12) are given by:

$$T_1 = T - g_T - \max\{0, g_L - \left(R_L + G_L + t_y\right)\}$$

$$T_2 = T_1 + g_{T1}$$

$$T_3 = T - G_T$$

$$T_4 = T_3 + \frac{g_{T1} \cdot n_T}{N_T}$$

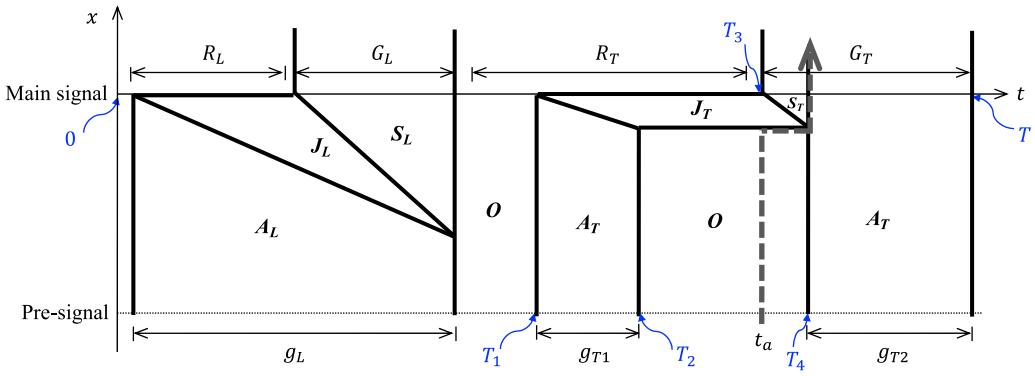

Fig. 3.12. Time-space diagram under pre-signal green truncation.

3.3.4 Solution method

Due to the many cases and complicated models revealed above, it would be tedious, if not impossible, to develop analytical solutions to the optimization problem (3.1). Thus, we use Monte Carlo simulation to generate numerous (> 10000) signal cycles, each with random bus arrival times. The optimal TSP parameters (G_{T0} for green extension, R'_T for red truncation, G_{L1}, R_{T1} and G_B for green insertion, and g_{T1} for pre-signal green truncation) are obtained for each cycle via exhaustive search. Expected car discharge capacity and bus delay as performance metrics are calculated by averaging cross the cycles.

3.4 Numerical analyses

We conduct extensive numerical analyses for a wide range of operating parameter values. Specifically, we let $N \in \{3,4,5\}$, $n = N - 1$, $\lambda_b \in \{30,90\}$ buses/hour, $l \in \{0.2,0.3\}$, $T = 120$ sec, $G = 60$ sec, $R_L = 14$ sec, $R_T = 34$ sec, $t_y = 3$ sec, and $q_S = 1800$ cars/hour. Other sets of parameter values were also tested, but the results are similar and thus omitted for brevity. For each set of parameter values, we compare the results for five scenarios: (i) under green extension scheme only; (ii) under red truncation only; (iii) under green insertion only; (iv) under pre-signal green truncation only; and (v) under the dynamic scheme specified in Section

3.2.3.5. Three benchmark scenarios are also compared: (vi) a "do-nothing" scenario where no pre-signal, bus lane or TSP is applied; (vii) a pre-signal only scenario where buses and cars are mixed and no TSP is applied; and (viii) an alternative dynamic scheme that is similar to the one used in scenario (v), except that a DBL is used throughout the shoulder lane. Under each of scenarios (i-v) and (viii), we plot the Pareto frontier between the expected T-car capacity and bus delay by varying the weight parameter r in the objective function (3.1) from 0 to 1.

Results for $l = 0.2$ are plotted in Fig. 3.13a-f. For the do-nothing scenario, the T-car discharge capacity has an upper bound that is attained if the bus flow is zero, and the expected bus delay reaches a lower bound when the car flow is zero. These two bounds are plotted as the grey square in the figures. Similarly, the same bounds for T-car capacity and expected bus delay under the pre-signal only scenario are plotted as the purple dot in those figures. In these figures, a curve closer to the upper-left corner is more Pareto-efficient.

Most importantly, the figures unveil that designs combining TSP schemes and the pre-signal (i.e., scenarios (i-v) and (viii)) always produce significantly higher car discharge capacity and lower bus delay than the do-nothing scenario (i). Thus, the integrated designs promote both bus and car traffic at busy intersection approaches. In addition, the design involving dynamic scheme (the dark blue curves) outperforms those involving a single type of TSP (the green, red, yellow, and brown curves) in both car capacity and bus delay saving. This design produces car capacities that are close to the upper bound attained by the pre-signal only scenario (vii). Meanwhile, it furnishes an average bus delay that is less than 10 seconds, and sometimes less than 5 seconds. On the other hand, the integrated design involving DBL (the light blue curves) can sometimes yield even lower bus delays, especially when the bus flow is high. This is as expected, since under the proposed design, buses will sometimes be impeded by T-car queues downstream in the sorting area, and thus experience more delays. However, the car capacity produced by the DBL design is lower than that of our proposed design. In practice, one can determine the value of r according to the relative preference between car capacity and bus delay savings, and select between the DBL design and the proposed design by comparing their objective function values.

Of note, the green insertion scheme seems to always outperform the other TSP schemes. This is because green insertion can prioritize a wider range of bus arrivals, without wasting much of the green time that may lead to car capacity loss.

Similar results are also observed for cases where $l = 0.3$, as illustrated in Fig. 3.14a-f.

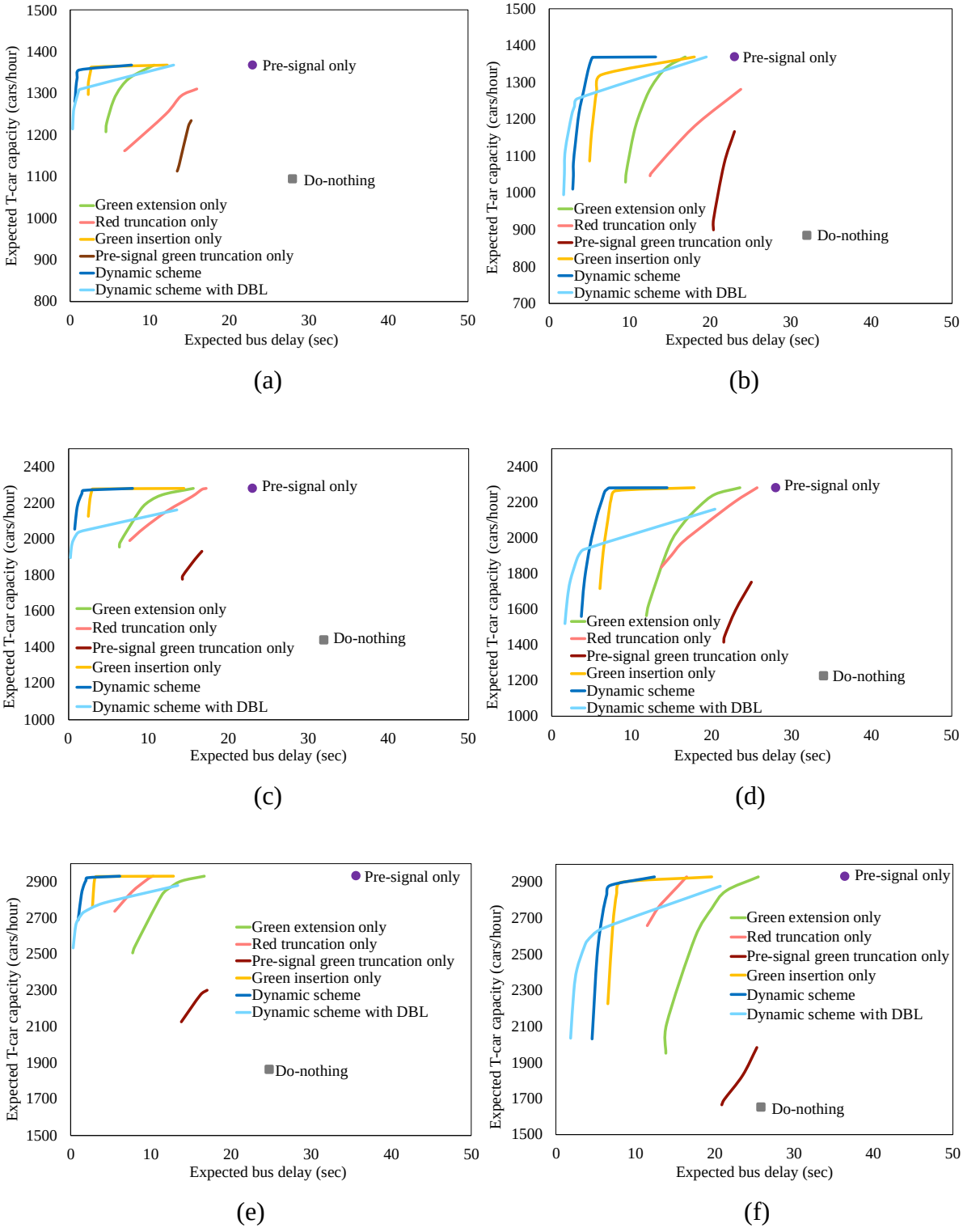

Fig. 3.13. $l = 0.2$: (a) $N = 3, \lambda_b = 30$ buses/hr; (b) $N = 3, \lambda_b = 90$ buses/hr; (c) $N = 4, \lambda_b = 30$ buses/hr; (d) $N = 4, \lambda_b = 90$ buses/hr; (e) $N = 5, \lambda_b = 30$ buses/hr; (f) $N = 5, \lambda_b = 90$ buses/hr.

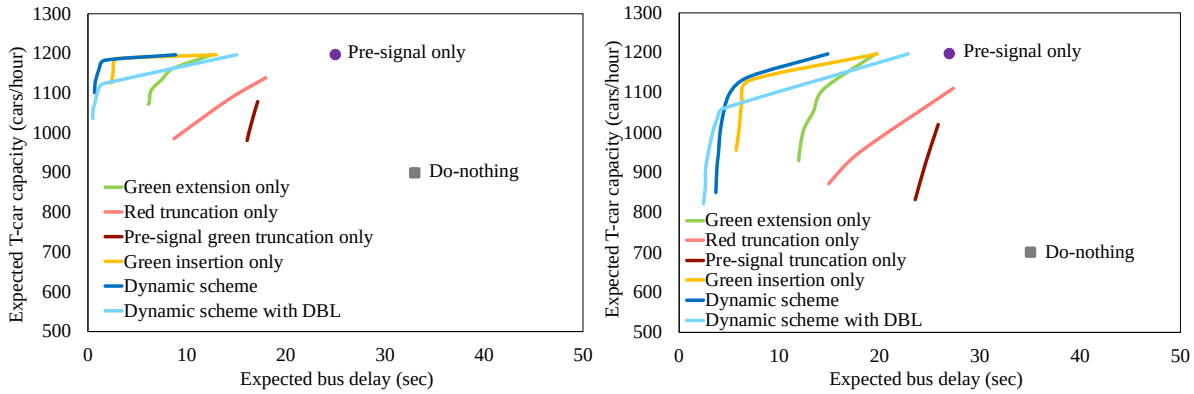

(a) (b)

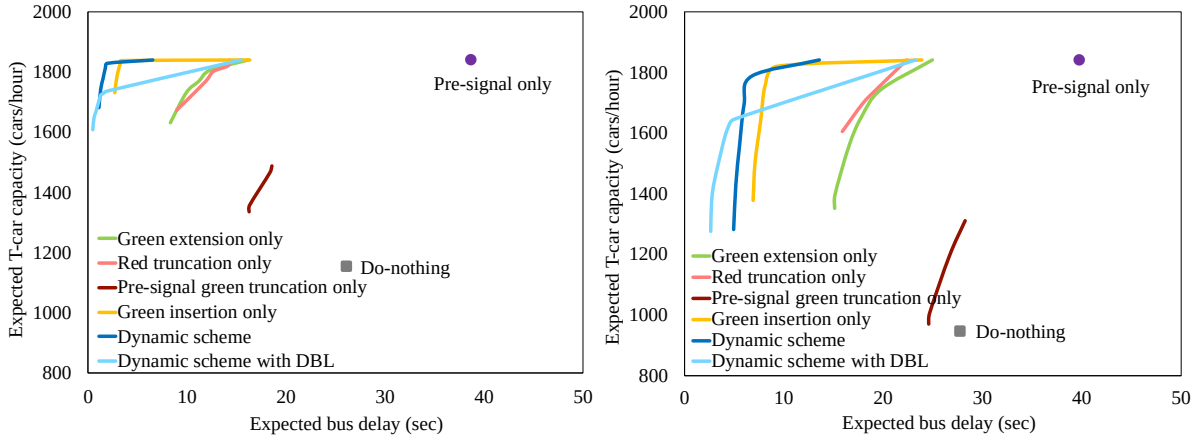

(c) (d)

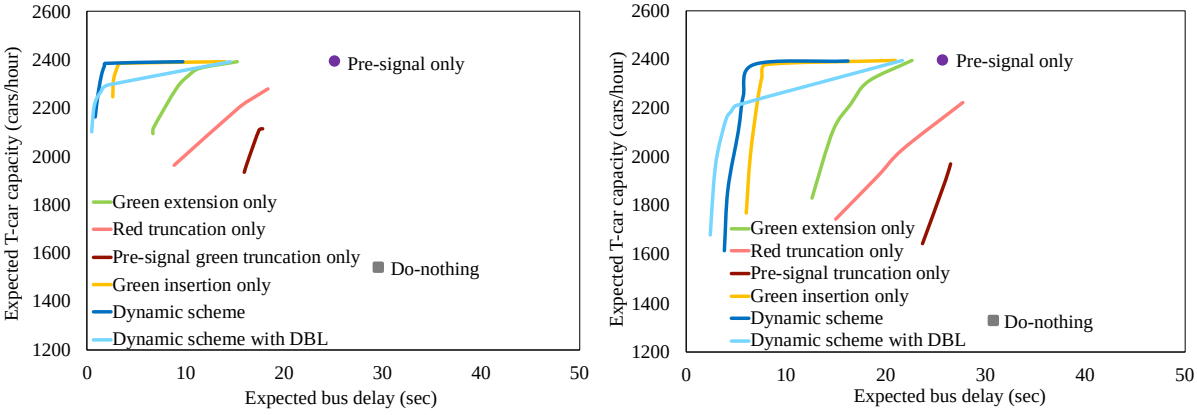

(e) (f)

Fig. 3.14. $l = 0.3$: (a) $N = 3, \lambda_b = 30$ buses/hr; (b) $N = 3, \lambda_b = 90$ buses/hr; (c) $N = 4, \lambda_b = 30$ buses/hr; (d) $N = 4, \lambda_b = 90$ buses/hr; (e) $N = 5, \lambda_b = 30$ buses/hr; (f) $N = 5, \lambda_b = 90$ buses/hr.

3.5 Summary

This chapter proposes a combined design of pre-signals, in conjunction with TSP schemes to improve the car discharge capacity of the intersection and at the same time prioritize buses. Four types of single TSP schemes as well as a dynamic strategy to choose the optimal one among the four schemes are considered. Analytical models are developed to calculate the bus delay and car capacity. Numerical results show that our proposed strategies can benefit both buses and cars concurrently under various operating conditions. We further compare our proposed design against the design of a dedicated bus lane, and two benchmark cases where only the pre-signal or none of the above design is implemented.

The results manifest the benefit of the proposed strategies and the capability of applying the models to dynamically coordinate the main- and pre-signal timings for improving the bimodal traffic operations at busy intersections. Note how the proposed design combine the two types of pre-signals to both sort through and left-turning car traffic in the tandem fashion, and allow buses to skip the car queues. Further note that our models are able to predict that under what conditions the DBL strategy performs better, and under what conditions the dynamic strategy with intermittent bus lane should be used.

Chapter 4

Conclusions

Section 4.1 summarizes the contributions of the thesis. Section 4.2 discusses the limitations and potential extensions of the present work.

4.1 Contributions

In this thesis, we develop optimal designs and operating strategies that favor transit performance at urban networks and signalized intersections. Major contributions are summarized as follows.

1. A parsimonious, continuous model is developed for transit systems where access and egress to or from transit stations can occur via shared-bikes, to minimize total travel costs. We consider a hybrid structure of transit networks, where transit lines form square grids inside city centers, and radiate outward in the peripheries. We allow patrons to choose between using shared-bikes and that of solely walking to or from transit stations. Note that shared-bikes are priced to achieve the system-optimal assignment of the two feeder options. For comparisons with other feeder options, similar models are built for systems in which access or egress to or from transit can occur solely by walking, or by walking and riding fixed-route feeder buses in combination.

2. Numerical studies of the transit-bike network are conducted for varying city size, travel demand, and economic conditions; and for trunk services that are provided either by ordinary buses, Bus Rapid Transit, or metro rail. Designs are produced for cases in which shared-bike and feeder-bus services are made to fit pre-existing and unchangeable trunk-line networks; and for cases in which trunk and feeder services are optimized jointly. Outcomes reveal that shared-bike feeder systems can virtually always reduce costs over walking alone, with cost savings as high as 7%, even when the shared bikes are made to fit a pre-existing transit network. Shared-biking often outperforms feeder-bus service as well. We further find that the joint optimization of trunk and shared-bike feeder services can reduce costs not only to users, but also to the transit agency that operates these services. Savings to the agency can be used to subsidize shared-bike services. We show that with or

without this subsidy, shared-bike systems can always break even when they are suitably priced, and jointly optimized with trunk service.

3. A pre-signal located upstream of the main intersection signal is deployed to increase car discharge capacity by sorting through-moving and left-turning cars, and at the same time to allow some buses to skip downstream car queues. This is integrated with five TSP schemes to provide extra transit priority. They are: green extension, red truncation, green insertion, pre-signal green truncation, and a dynamic scheme that selects the optimal scheme among the above four for each cycle. We show how the pre-signal can be operated to coordinate with the main signal in all proposed schemes.

4. Analytical models are formulated to calculate two performance metrics for an intersection approach under the proposed designs, i.e., the expected car discharge capacity and expected bus delay. Pareto frontiers are obtained by optimizing the trade-off between these two metrics. Numerical results show that all the proposed designs can benefit both buses and cars concurrently under various operating conditions. The dynamic scheme always outperforms the four single-type TSP schemes by a considerable margin. The results manifest the benefit of the proposed designs. Comparison with an alternative design with DBL reveals the conditions under which each design (i.e., with proposed design or DBL) wins.

4.2 Discussion and future work

Future research can be conducted by addressing the following issues:

1. Regarding joint optimization of transit and shared-bike networks, present findings come by means of simplified models for idealized cases. In some instances, the simplifications are conservative; e.g. recall that some short-distance commuters might enjoy greater cost savings by using shared bikes to cover their entire trips. This might justify trunk designs with larger line and station spacings (to serve longer-distance trips). The benefits might trigger favorable modal shifts, which could benefit transit, and was likewise not considered in the present study. This can be done by incorporating mode (and route) choice models of deterministic or stochastic (e.g., logit) kind.

2. New design models for transit networks fed by shared bikes or other faster access modes (e.g., electrical scooters, autonomous cars providing ride sharing service) can also be developed to account for greater realism, e.g., spatially heterogeneous demand. Consideration of demand heterogeneity may entail the use of continuum approximation techniques (e.g. Chien and Schonfeld, 1997; Ouyang et al., 2014).

3. Our present work on bimodal traffic at signalized intersections assumes all buses make through movement for simplicity. Future research can include left-turning buses by refining the holding mechanism at the pre-signal to allow the left-turning buses to switch to the innermost lane without being impeded by car queues.

4. The focus of this work is on oversaturated car traffic at signalized intersections. Increasing discharge capacity can reduce the number of cars that wait for multiple cycles to pass the intersection, as well as their delays. However, the delay analysis for the undersaturated car traffic is omitted in this thesis. In reality, no intersection would be oversaturated all the time, and undersaturated situations need to be addressed in future work.

5. The analysis in this work assumes the saturation headway of car traffic is deterministic. In reality, vehicles discharged in a given signal cycle is not a constant number. The stochastic saturation headways may result in residual car queues and capacity loss. We believe that residual queues can be detected by loop detectors or roadside sensors immediately. Once a residual queue is detected, we would shorten the green time at pre-signal to avoid overcrowding in the sorting area. The pre-signal timing plan would resume after the residual queues have dissipated.

6. The pre-signal analysis in this work implicitly assumes that drivers will always comply with the lane assignment imposed by our proposed design. However, non-compliance driver behaviors can result in residual queues in the sorting area, and discharge capacity of the intersection could be significantly reduced. For example, if a through-moving vehicle taking the left-turning lane to jump the queue, this T-vehicle will not turn left and may block the L-vehicles behind it from turning left. To address non-compliance behaviors, variable message signs can be added upstream of the pre-signal to remind car drivers to conform to the dynamic lane assignment rule of the pre-signal (Luo, 2011).

7. The work on a single intersection can be extended to model a signalized arterial with multiple intersections. Coordination between consecutive signals will be considered. The reliability of bus service, in terms of, e.g., schedule adherence, can be accounted for in addition to bus delays. This means sometimes delaying a bus purposely at the intersection could be beneficial.

8. We also plan to study designs and strategies to promote bimodal traffic at narrow intersection approaches, e.g., one with only two lanes. In this case, the pre-signal can be used to manage lane changes for cars, so that a coming bus can utilize an empty lane to jump the car queues.

Appendices

A. Tables of notations

A.1 Table of notations in Chapter 2

Notation	Description	Unit
Decision variables		
α	Ratio between the sides of central square and the city in the hybrid transit network	-
P	Density of small bike docking stations	station/km^2
H_k	Trunk-line transit headway in period k, $k \in \{p, o\}$	h
$H_{f,k}$	Feeder-bus headway in period k, $k \in \{p, o\}$	h
S	Trunk-line transit station spacing	km
S_f	Feeder-bus line and stop spacing	km
Other variables and parameters		
β	Percentage of able-bodied persons in the city's transit patrons	-
ρ	Bike utilization ratio during peak periods	-
μ	Patrons' value of time	\$/h
t_k	Peak/off-peak period duration of a day, $k \in \{p, o\}$	h
λ	Average demand density during the service hours of a day	trips/h/km^2
D	Length (and width) of the square city	km
v	Trunk-line transit vehicle cruise speed	km/h
v_f	Feeder-bus cruise speed	km/h
v_w	Walking speed	km/h
v_b	Cycling speed	km/h
δ	Equivalent walking time for a transfer between two perpendicular trunk transit lines	h
t_f	Intermodal transfer penalty	h
τ_f	Feeder-bus dwell time per stop	h
τ	Trunk-line transit vehicle dwell time per station	h
t_{dp}	Bike pick-up delay at the origin docking station	h
t_{dd}	Bike drop-off delay at the destination docking station	h
C_I	Amortized hourly cost rate of trunk-line transit infrastructure	\$/h/km
C_S	Amortized hourly cost rate of trunk-line transit station	\$/h/station
C_{VD}	Distance-based operating cost rate of trunk-line transit	\$/vehicle-km
C_{VT}	Time-based operating cost rate of trunk-line transit	\$/vehicle-h
C_{fI}	Amortized hourly cost rate of feeder-bus line infrastructure	\$/h/km
C_{fS}	Amortized hourly cost rate of a feeder-bus stop	\$/h/stop
C_{fVD}	Distance-based operating cost rate of feeder bus	\$/bus-km
C_{fVT}	Time-based operating cost rate of feeder bus	\$/bus-h
C_B	Daily cost per bike	\$/bike/day

Notation	Description	Unit
C_D	Daily cost per dock	\$/dock/day
C_P	Daily cost per docking station	\$/station/day
n_B	Average bike hours used per patron during peak periods	h
ξ	Ratio between the numbers of docks and bikes	-
$UC_{W,k}$	Average patron cost per trip in period k for access solely by walking, $k \in \{p, o\}$	h
$UC_{B,k}$	Average patron cost per trip in period k for access by cycling and walking, $k \in \{p, o\}$	h
$UC_{F,k}$	Average patron cost per trip in period k for access by feeder buses and walking, $k \in \{p, o\}$	h
$E_{T,k}$	Sum of average wait, in-vehicle travel time and transfer penalty per trip in period k, $k \in \{p, o\}$	h
t_w	Average walking time to the nearest bike docking station for each cycling trip	h
t_r	Average in-vehicle travel time by feeder bus for each feeder-bus trip	h
$E_{B,k}$	Average access and egress time per trip via bike in period k, $k \in \{p, o\}$	h
$E_{F,k}$	Average access and egress time per trip via feeder bus in period k, $k \in \{p, o\}$	h
AC_k	Average trunk-line transit agency cost per trip in period k, $k \in \{p, o\}$	h
$\$_I$	Amortized (trunk) transit line infrastructure cost per hour per km^2	\$/h/km^2
$\$_S$	Amortized (trunk) transit station cost per hour per km^2	\$/h/km^2
$\$_{VD,k}$	Distance-based (trunk) transit operating cost per hour per km^2 in period k, $k \in \{p, o\}$	\$/h/km^2
$\$_{VT,k}$	Time-based (trunk) transit operating cost per hour per km^2 in period k, $k \in \{p, o\}$	\$/h/km^2
AC_B	Average bike-sharing agency cost per trip	h
$AC_{F,k}$	Average feeder-bus agency cost per trip in period k, $k \in \{p, o\}$	h
K	Trunk-line transit vehicle's passenger-carrying capacity	passenger/vehicle
K_f	Feeder bus's passenger-carrying capacity	passenger/bus
MC_{B-W}	Marginal generalized cost when a patron switches from walking to cycling at one end of her trip	h
MAC_B	Marginal bike-sharing agency cost when a patron switches from walking to cycling at one end of her trip	\$
MC_{F-W}	Marginal generalized cost when a patron switches from walking to feeder bus at one end of her trip	h
MAC_F	Marginal feeder-bus agency cost when a patron switches from walking to feeder bus at one end of her trip	\$
d_w	Average distance to the nearest bike docking station	km
d_{ck}	Critical distance between walking and cycling in period k, $k \in \{p, o\}$	km
d_{ck1}	Critical distance between walking and taking feeder bus in the non-stop direction in period k, $k \in \{p, o\}$	km

Notation	Description	Unit
d_{ck2}	Critical distance between walking and taking feeder bus in the passenger-collection direction in period k, $k \in \{p, o\}$	km
φ_k	Distance-based bike rental fee in period k, $k \in \{p, o\}$	$
γ_k	Bike rental rate in period k, $k \in \{p, o\}$	$/km
$A_{fw,k}$	Area of the walk-only region in period k for access by feeder buses and walking, $k \in \{p, o\}$	km^2
$A_{bw,k}$	Area of the walk-only region in period k for access by cycling and walking, $k \in \{p, o\}$	km^2
$d_{bin,k}$	Average access distance in the walk-only region in period k for access by cycling and walking, $k \in \{p, o\}$	km
$d_{bout,k}$	Average access distance in the cycling region in period k, $k \in \{p, o\}$	km
$d_{fin,k}$	Average access distance in the walk-only region in period k for access by feeder buses and walking, $k \in \{p, o\}$	km
$d_{fout1,k}$	Average access distance in the non-stop direction in the feeder-bus region in period k, $k \in \{p, o\}$	km
$d_{fout2,k}$	Average access distance in the passenger-collection direction in the feeder-bus region in period k, $k \in \{p, o\}$	km
R	Bike rental revenue	$/day/km^2

A.2 Table of notations in Chapter 3

Notation	Definition
T	Signal cycle length
G	Total duration of main signal green phases
G_L, G_T	Durations of main signal green phases for L- and T- traffic, respectively
R_L, R_T	Durations of main signal red phases for L- and T- traffic, respectively
g_L, g_T	Durations of pre-signal green phases for L- and T- traffic, respectively
N	Total number of car lanes at main signal
N_L, N_T	Numbers of L- and T- car lanes at main signal, respectively
n	Total number of car lanes at pre-signal
n_L, n_T	Numbers of L- and T- car lanes at pre-signal, respectively
l	Left-turning ratio
t_y	Amber time
t_a	Arrival time for the a^{th} bus
G_{T0}	Extended green time in green extension scheme
t_R	Redundant green time for G_T phase
R_T'	Truncated red phase in red truncation scheme
G_B	Inserted green time in green insertion scheme
G_{L1}, G_{L2}	Partitioned G_L phases in green insertion scheme

R_{T1}, R_{T2}	Partitioned R_T phases in green insertion scheme
g_{T1}, g_{T2}	Truncated g_T phases in pre-signal green truncation scheme
λ_b	Poisson arrival rate for buses
δ	Passenger car equivalent of a bus
m	Number of buses arriving in a signal cycle
D_B	Total bus delay in a signal cycle
$d_b(t_a)$	Bus delay for the a^{th} arriving bus
q_s	Capacity of a car lane in the subject approach
$Q(N, n)$	Capacity at an intersection with N lanes at main signal and n lanes at pre-signal
Q_T	Maximum number of T-cars that can discharged in a signal cycle
W	Objective function to optimize TSP schemes
r	Weighting ratio for total bus delay
A_L, A_T	Discharge flows from the pre-signal for L- and T- traffic, respectively
S_L, S_T	Saturated flow states at main signal for L- and T- traffic, respectively
J_L, J_T	Jam states at main signal for L- and T- traffic, respectively
w, w_L and w_T	Shockwave speeds

B. Proof of Proposition 2.1

To see why the diamond grid is the optimal layout of bike docking stations, note in Fig. B.1 that under this layout the boundary of a station's catchment zone are the isodistance lines in the L_1-metric for the distance $\sqrt{\frac{1}{2P}}$. Thus, a catchment zone of the same area ($\frac{1}{P}$ km^2) but with a different shape (see the one enclosed by a solid black boundary in the figure) will always have a larger average access distance to the docking station. Note that the cross-hatched parts in Fig. B.1, which belong to an arbitrary-shaped catchment zone but not to the diamond zone, are located outside of the isodistance lines, and thus have an average access distance greater than $\sqrt{\frac{1}{2P}}$. In contrast, the linear-hatched parts, which belong to the diamond zone but not to the arbitrary-shaped one, have an average access distance less than $\sqrt{\frac{1}{2P}}$. ■

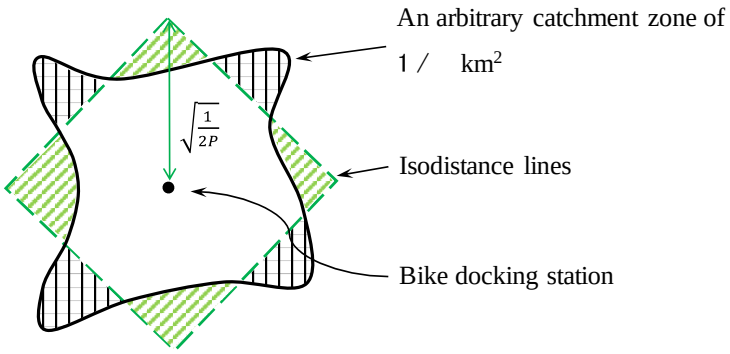

Fig. B.1. An arbitrary catchment zone versus a diamond zone with the same area.

C. Derivation of $d_{ck}, A_{bw,k}, d_{bin,k}$, and $d_{bout,k} (k \in \{p, o\})$.

We first derive the critical distance, d_{ck} $(k \in \{p, o\})$, by solving the equation $MC_{B-W} = 0$. From (2.8a) and (2.8b), we know that for off-peak periods:

$$d_{co} \equiv \frac{\frac{1}{v_w}\sqrt{\frac{2}{9P}} + t_{dp} + t_{dd} + t_f}{\frac{1}{v_w} - \frac{1}{v_b}}; \tag{C1}$$

and for peak periods when $\frac{1}{v_w} > \frac{1}{v_b} + \frac{C_B + \xi C_D}{\mu \rho t_p v_b}$:

$$d_{cp} = \frac{\frac{C_B + \xi C_D}{\mu \rho t_p}(t_{dp} + t_{dd}) + \frac{1}{v_w}\sqrt{\frac{2}{9P}} + t_{dp} + t_{dd} + t_f}{\frac{1}{v_w} - \frac{1}{v_b} - \frac{C_B + \xi C_D}{\mu \rho t_p v_b}}. \tag{C2}$$

For peak periods when $\frac{1}{v_w} \leq \frac{1}{v_b} + \frac{C_B + \xi C_D}{\mu \rho t_p v_b}$, $MC_{B-W} > 0$ for all non-negative values of d. In this case, we set $d_{cp} = S$.

In each period (peak or off-peak), the isodistance lines at d_{ck} divide the catchment zone of a transit station into the walk-only region $(d \leq d_{ck})$ and the cycling region $(d > d_{ck})$. Depending on the value of $\frac{d_{ck}}{S}$, the walk-only region can take one of the three shapes as shown in Fig. 2.3a-c. The $A_{bw,k}$ and $d_{bin,k} (k \in \{p, o\})$ are developed for each case as follows:

(i) When $\frac{d_{ck}}{S} \leq \frac{1}{2}$, the walk-only region has a diamond shape (see Fig. 2.3a). Thus we have:

$A_{bw,k} = 2d_{ck}^2$;

$d_{bin,k} = \frac{4\int_0^{d_{ck}} dx \int_0^{d_{ck}-x}(x+y)dy}{A_{bw,k}} = \frac{2}{3}d_{ck}$.

(ii) When $\frac{1}{2} < \frac{d_{ck}}{S} < 1$, the walk-only region is an octagon (see Fig. 2.3b). By geometry, we have:

$A_{bw,k} = 2d_{ck}^2 - 4\left(d_{ck} - \frac{S}{2}\right)^2$;

$d_{bin,k} = \frac{\frac{2}{3}d_{ck}\cdot 2d_{ck}^2 - 8\int_0^{d_{ck}-\frac{S}{2}} dx \int_{\frac{S}{2}}^{d_{ck}-x}(x+y)dy}{A_{bw,k}} = \frac{\frac{2}{3}d_{ck}\cdot 2d_{ck}^2 - 8\left(\frac{2}{3}d_{ck}+\frac{S}{6}\right)\cdot\frac{1}{2}\left(d_{ck}-\frac{S}{2}\right)^2}{A_{bw,k}}$;

(iii)When $\frac{d_{ck}}{S} \geq 1$, the walk-only region fills up the entire catchment zone (see Fig. 2.3c). Thus, $A_{bw,k} = S^2$; $d_{bin,k} = \frac{S}{2}$.

In all the three cases, $d_{bout,k} = \frac{\frac{S}{2}\cdot S^2 - d_{bin,k}\cdot A_{bw,k}}{S^2 - A_{bw,k}}$. Specifically, in case (iii), $d_{bout,k} = 0$.

D. Proof of Proposition 2.3

Equations (2.7a) and (2.7b) reveal that an able-bodied patron in period $k \in \{p, o\}$ with access distance d will choose walking if $u_{Bk}(d) - u_{Wk}(d) = \left(\frac{d}{v_b} + t_w + t_{dp} + t_{dd} + t_f + \frac{\varphi_k(d)}{\mu}\right) - \frac{d}{v_w} > 0$, and will choose cycling otherwise. From Proposition 2.2, we know the following conditions should be satisfied for system-optimal pricing:

$$\begin{cases} \frac{d}{v_w} < \left(\frac{d}{v_b} + t_w + t_{dp} + t_{dd} + t_f\right) + \frac{\varphi_k(d)}{\mu}, & if\ 0 \leq d < d_{ck} \\ \frac{d_{ck}}{v_w} = \left(\frac{d_{ck}}{v_b} + t_w + t_{dp} + t_{dd} + t_f\right) + \frac{\varphi_k(d_{ck})}{\mu}, & if\ d = d_{ck} \\ \frac{d}{v_w} > \left(\frac{d}{v_b} + t_w + t_{dp} + t_{dd} + t_f\right) + \frac{\varphi_k(d)}{\mu}, & if\ d_{ck} < d \leq S \end{cases} \qquad k \in \{p, o\}. \tag{D1}$$

Mathematically, the middle equation of (D1) does not need to hold for a system-optimal pricing scheme; i.e., at the critical distance, a patron can choose either walking or cycling, and the costs of the two access modes do not have to be equal. However, we keep this equation for the simplicity of derivation. Since d_{ck} is the root of $MC_{B-W} = 0$, we have:

$$\varphi_k(d_{ck}) = MAC_B = \begin{cases} \frac{C_B+\xi C_D}{\rho t_p}\left(\frac{d_{ck}}{v_b} + t_{dp} + t_{dd}\right), & \text{for } k = p \\ 0, & \text{for } k = o. \end{cases} \quad \text{(D2)}$$

By subtracting the middle equation of (D1) from the first and third inequalities of (D1), we have:

$$\begin{cases} \frac{d-d_{ck}}{v_w} < \frac{d-d_{ck}}{v_b} + \frac{\varphi_k(d)-\varphi(d_{ck})}{\mu} & \text{if } 0 \le d < d_{ck} \\ \frac{d-d_{ck}}{v_w} > \frac{d-d_{ck}}{v_b} + \frac{\varphi_k(d)-\varphi(d_{ck})}{\mu} & \text{if } d_{ck} < d \le S. \end{cases} \quad \text{(D3)}$$

We only need to show that there exists $\varphi_k(d)$ for period $k \in \{p, o\}$ that satisfies (D2) and (D3). In addition, a feasible fee scheme, $\varphi_k(d)$, should generally be: (i) non-negative for all the $d \in [0, S]$; and (ii) non-decreasing as d increases. To show the existence of a feasible system-optimal fee scheme, we consider a special case: a scheme where the fee increases linearly with the distance traveled. This linear fee scheme is expressed by $\varphi_k(d) - \varphi_k(d_{ck}) = \gamma_k(d - d_{ck})$ $(k \in \{p, o\})$, where γ_k is a non-negative constant rate for period k, and $\varphi_k(d_{ck})$ is given by (D2). This linear fee scheme is non-decreasing as d grows and satisfies (D3) if $0 \le \gamma_k < \mu\left(\frac{1}{v_w} - \frac{1}{v_b}\right)$. To ensure $\varphi_k(d)$ is non-negative for all the $d \in [0, S]$, we modify the definition of $\varphi_k(d)$ to the following:

$$\varphi_k(d) = \max\{0, \gamma_k(d - d_{ck}) + \varphi_k(d_{ck})\},\ 0 \le \gamma_k < \mu\left(\frac{1}{v_w} - \frac{1}{v_b}\right),\ k \in \{p, o\}. \quad \text{(D4)}$$

The above modification will not alter any patron's access choice, because a negative $\gamma_k(d - d_{ck}) + \varphi_k(d_{ck})$ may occur only when $d < d_{ck}$ (i.e. in the walk-only region). ■

E. Derivation of $A_{fw,k}$ and $E_{F,k}$ $(k \in \{p, o\})$

We again consider a patron whose access distance is d $(0 \le d \le S)$. The marginal generalized cost incurred to the system when the patron switches from walking to riding a feeder bus is:

$$MC_{F-W} = \left(\frac{S_f}{2v_w} + \frac{H_{f,k}}{2} + t_r + t_f + \frac{MAC_F}{\mu}\right) - \frac{d}{v_w}, \quad \text{(E1)}$$

where $\frac{S_f}{2v_w}$ denotes the (average) walking time from the patron's origin to the nearest feeder bus station; $\frac{H_{f,k}}{2}$ the (average) time spent to wait for a feeder bus at the origin station; t_r the travel

time in the feeder bus; t_f the intermodal transfer penalty between feeder bus and trunk transit; and MAC_F the marginal feeder bus agency cost (in \$) added to the system for serving this additional feeder passenger. At the system optimum, the patron will choose a feeder bus if and only if $MC_{F-W} < 0$, and will choose walking otherwise. Therefore, we can again obtain the system-optimal access mode assignment by solving $MC_{F-W} = 0$. To solve this equation, we need to derive MAC_F and t_r.

To simplify the derivation of MAC_F, we assume that a feeder bus always has sufficient capacity to accommodate its patrons. This is usually true because a feeder bus serves a small local zone only (and we have verified in all the numerical instances in this thesis that the feeder bus capacity constraint (2.10b) is never binding). Under this assumption, adding a new passenger to the feeder network will not incur any extra agency cost, which means $MAC_F = 0$. Note that this also means the system-optimal feeder-bus fare can be set to zero.

The t_r is the sum of two parts: the in-vehicle travel time along the non-stop route segment, $t_{r1} = \frac{d_1}{v_f}$, and the in-vehicle travel time along the route segment when collecting passengers, $t_{r2} = d_2\left(\frac{1}{v_f} + \frac{\tau_f}{S_f}\right)$. Here d_1 and d_2 are the patron's access distances along the two perpendicular segments, respectively; v_f denotes the feeder bus's cruise speed; and τ_f denotes the bus dwell time at a feeder bus stop. Hence, two critical distances will be developed by solving $MC_{F-W} = 0$: by setting $d_2 = 0$, we find the critical distance, d_{ck1} $(k \in \{p, o\})$, in the non-stop travel direction; and by setting $d_1 = 0$, we find the critical distance, d_{ck2} $(k \in \{p, o\})$, in the passenger-collection direction. They are:

$$\begin{cases} d_{ck1} = \dfrac{\frac{S_f}{2v_W} + \frac{H_{f,k}}{2} + t_f}{\frac{1}{v_W} - \frac{1}{v_f}} \\ d_{ck2} = \dfrac{\frac{S_f}{2v_W} + \frac{H_{f,k}}{2} + t_f}{\frac{1}{v_W} - \frac{1}{v_f} - \frac{\tau_f}{S_f}} \end{cases}, \quad k \in \{p, o\}. \tag{E2}$$

This means that the isodistance lines from the trunk station form an anisotropic diamond, as shown by the thin, solid lines in Fig. E.1a-d. (Note that d_{ck1} is always smaller than d_{ck2}.) As a result, four cases may arise regarding the shape of the walk-only region, as illustrated in Fig. E.1a-d. They are: when $\frac{d_{ck1}}{S}, \frac{d_{ck2}}{S} \leq \frac{1}{2}$; when $\frac{d_{ck1}}{S} \leq \frac{1}{2}, \frac{d_{ck2}}{S} > \frac{1}{2}$; when

$\frac{d_{ck1}}{S}, \frac{d_{ck2}}{S} > \frac{1}{2}$ and $\frac{d_{ck1}d_{ck2}}{d_{ck1}+d_{ck2}} \leq \frac{S}{2}$; and when $\frac{d_{ck1}d_{ck2}}{d_{ck1}+d_{ck2}} > \frac{S}{2}$. In each figure, the trunk station is marked by the black dot and its catchment zone is bounded by the dashed square; the thick solid lines represent the trunk lines as they would be laid-out in a grid network; and the walk-only region is shaded.

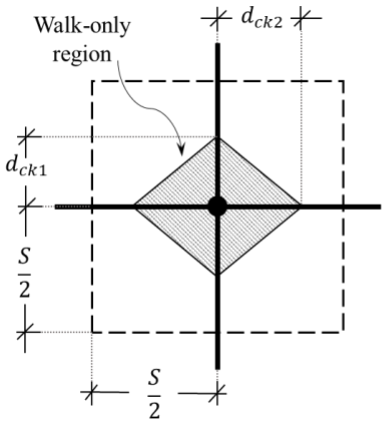

(a) when $\frac{d_{ck1}}{S}, \frac{d_{ck2}}{S} \leq \frac{1}{2}$

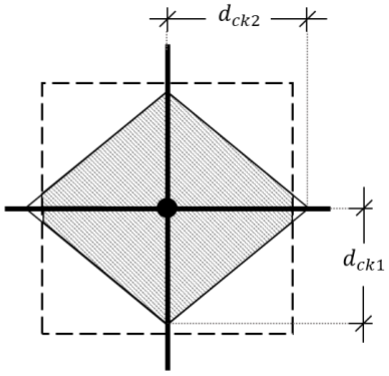

(b) when $\frac{d_{ck1}}{S} \leq \frac{1}{2}, \frac{d_{ck2}}{S} > \frac{1}{2}$

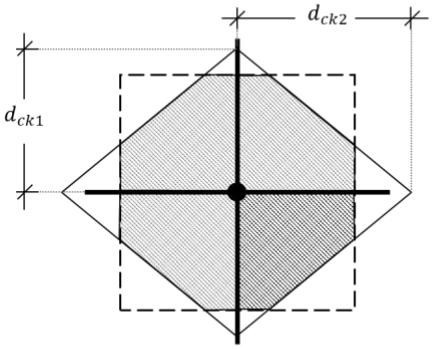

(c) when $\frac{d_{ck1}}{S}, \frac{d_{ck2}}{S} > \frac{1}{2}$ and $\frac{d_{ck1}d_{ck2}}{d_{ck1}+d_{ck2}} \leq \frac{S}{2}$

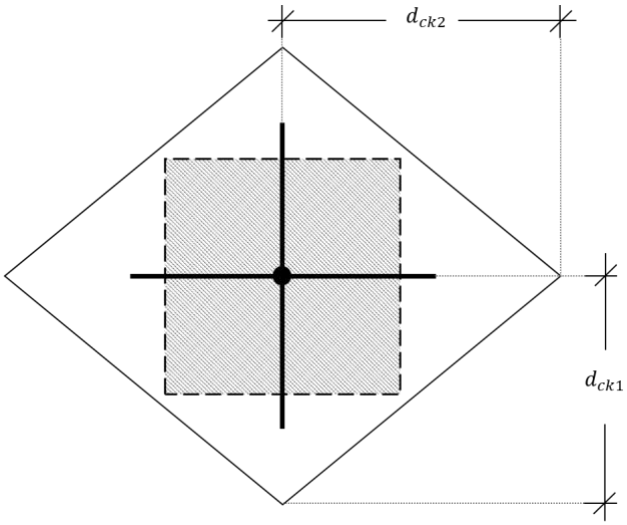

(d) when $\frac{d_{ck1}d_{ck2}}{d_{ck1}+d_{ck2}} > \frac{S}{2}$

Fig. E.1. The walk-only region in the catchment zone of a trunk station in period $k \in \{p, o\}$.

For each of the four cases shown in Fig. E.1a-d, we define $A_{fw,k}$ $(k \in \{p, o\})$ as the area of the walk-only region in period k; and $d_{fin,k}$ as the average access distance in that region during k. In the feeder-bus region, we define two average access distances, $d_{fout1,k}$ and

$d_{fout2,k}$, for the non-stop trip portion and the passenger-collection portion, respectively. The $E_{F,k}$ is calculated as:

$$E_{F,k} = 2\left(\frac{A_{fw,k}}{S^2}\cdot\frac{d_{fin,k}}{v_w} + \left(1-\frac{A_{fw,k}}{S^2}\right)\left(\frac{d_{fout1,k}}{v_f} + d_{fout2,k}\cdot\left(\frac{1}{v_f}+\frac{\tau_f}{S_f}\right) + \frac{S_f}{2} + \frac{H_{f,k}}{2} + t_f\right)\right), \quad k \in \{p, o\}. \tag{E3}$$

The $A_{fw,k}$, $d_{fin,k}$, $d_{fout1,k}$ and $d_{fout2,k}$ $(k \in \{p, o\})$ are developed for each case shown in Fig. E.1a-d as follows:

(i) When $\frac{d_{ck1}}{S}, \frac{d_{ck2}}{S} \le \frac{1}{2}$, the walk-only region has a diamond shape (see Fig. E.1a). Thus, we have:

$$A_{fw,k} = 2d_{ck1}d_{ck2};$$

$$d_{fin,k} = \frac{4\int_0^{d_{ck2}} dx \int_0^{d_{ck1}-\frac{d_{ck1}}{d_{ck2}}x} (x+y)dy}{A_{fw,k}} = \frac{d_{ck1}+d_{ck2}}{3};$$

$$d_{fout1,k} = d_{fout2,k} = \frac{S^2+2d_{ck1}d_{ck2}}{4S}.$$

(ii) When $\frac{d_{ck1}}{S} \le \frac{1}{2}, \frac{d_{ck2}}{S} > \frac{1}{2}$, the walk-only region is a hexagon (see Fig. E.1b). Thus, we have:

$$A_{fw,k} = S\cdot\left(2d_{ck1} - \frac{d_{ck1}\cdot S}{2d_{ck2}}\right);$$

$$d_{fin,k} = \frac{2d_{ck1}d_{ck2}\cdot\left(\frac{d_{ck1}+d_{ck2}}{3}\right) - 4\int_{\frac{S}{2}}^{d_{ck2}-\frac{S}{2}} dx \int_0^{d_{ck1}-\frac{d_{ck1}}{d_{ck2}}x} (x+y)dy}{A_{fw,k}}$$

$$= \frac{2d_{ck2}(d_{ck1}+S) - (d_{ck2}-S)\left(\frac{d_{ck1}}{d_{ck2}}-d_{ck1}-S\right)}{3d_{ck2}\left(2-\frac{S}{2d_{ck2}}\right)};$$

$$d_{fout1,k} = \frac{\left(d_{ck1}+\frac{S}{2}\right)}{2} + \frac{\left(d_{ck1}-\frac{d_{ck1}}{d_{ck2}}\frac{S}{2}+\frac{S}{2}\right)}{2} = \frac{2d_{ck1}-\frac{d_{ck1}}{d_{ck2}}\frac{S}{2}+S}{4};$$

$$d_{fout2,k} = \frac{\left(\frac{S}{2}+\frac{S}{4}\right)}{2} \cdot \frac{\frac{d_{ck1}\cdot\frac{S}{2}}{d_{ck2}}}{\left(\frac{S}{2}+\frac{d_{ck1}\cdot\frac{S}{2}}{d_{ck2}}-d_{ck1}\right)} + \frac{S}{4} \cdot \frac{\left(\frac{S}{2}-d_{ck1}\right)}{\left(\frac{S}{2}+\frac{d_{ck1}\cdot\frac{S}{2}}{d_{ck2}}-d_{ck1}\right)}$$

$$= \frac{\frac{3S^2\cdot d_{ck1}}{16d_{ck2}}+\frac{S^2}{8}-\frac{S}{4}\cdot d_{ck1}}{\left(\frac{S}{2}+\frac{d_{ck1}\cdot\frac{S}{2}}{d_{ck2}}-d_{ck1}\right)}.$$

(iii) When $\frac{d_{ck1}}{S}, \frac{d_{ck2}}{S} > \frac{1}{2}$ and $\frac{d_{ck1}d_{ck2}}{d_{ck1}+d_{ck2}} \leq \frac{S}{2}$, the walk-only region is an octagon (see Fig. E.1c). Thus, we have:

$$A_{fw,k} = 2d_{ck1}\cdot S - \frac{d_{ck1}\cdot S^2}{2d_{ck2}} + 2d_{ck2}\cdot S - \frac{d_{ck2}\cdot S^2}{2d_{ck1}} - 2d_{ck1}d_{ck2};$$

$$d_{fin,k} = \frac{2d_{ck1}d_{ck2}\cdot\left(\frac{d_{ck1}+d_{ck2}}{3}\right) - 4\int_{\frac{S}{2}}^{d_{ck2}-\frac{S}{2}} dx \int_0^{d_{ck1}-\frac{d_{ck1}}{d_{ck2}}x} (x+y)dy - 4\int_0^{d_{ck2}-\frac{d_{ck2}\cdot S}{2d_{ck1}}} dx \int_{\frac{S}{2}}^{d_{ck1}-\frac{d_{ck1}}{d_{ck2}}x} (x+y)dy}{A_{fw,k}}$$

$$= \frac{d_{ck1}d_{ck2}(4S-4d_{ck1}-2d_{ck2}+3d_{ck2}\cdot S)+S\left(2{d_{ck1}}^2+2d_{ck1}\cdot S-3{d_{ck2}}^2\cdot S\right)+\frac{d_{ck1}\cdot S}{d_{ck2}}\left(\frac{d_{ck1}\cdot S}{d_{ck2}}d_{ck1}-S^2\right)+\frac{d_{ck2}\cdot S^2}{4d_{ck1}}(d_{ck2}\cdot S+6d_{ck2}-S)}{3\left(2d_{ck1}\cdot S-\frac{d_{ck1}\cdot S^2}{2d_{ck2}}+2d_{ck2}\cdot S-\frac{d_{ck2}\cdot S^2}{2d_{ck1}}-2d_{ck1}d_{ck2}\right)};$$

$$d_{fout1,k} = \frac{\frac{S}{2}+\frac{\left(\frac{\left(d_{ck1}-\frac{S}{2}\right)\cdot d_{ck2}}{d_{ck1}}+\frac{S}{2}\right)}{2}}{2} = \frac{\frac{3S}{2}\cdot d_{ck1}+\left(d_{ck1}-\frac{S}{2}\right)\cdot d_{ck2}}{4d_{ck1}};$$

$$d_{fout2,k} = \frac{\frac{S}{2}+\frac{\left(\frac{S}{2}-\frac{d_{ck1}\cdot\frac{S}{2}}{d_{ck2}}+d_{ck1}\right)}{2}}{2} = \frac{3S-\frac{d_{ck1}}{d_{ck2}}\cdot S+2d_{ck1}}{8}.$$

(iv) When $\frac{d_{ck1}d_{ck2}}{d_{ck1}+d_{ck2}} > \frac{S}{2}$, the walk-only region fills up the entire catchment zone of the transit station (see Fig. E.1d). Thus, we have: $A_{fw,k} = S^2$, $d_{fin,k} = \frac{S}{2}$ and $d_{fout1,k} = d_{fout2,k} = 0$.

F. Bike-sharing cost rates

Cost rates for bike-sharing systems were derived by considering both the capital and the operating costs. The former include the purchase and installation fees for bikes, individual docks, and bike docking stations; and the latter consist of maintenance, repair and replacement, system management (including bike redistribution), and insurance fees for bikes and docking stations (Gleason and Miskimins, 2012). In this appendix, we provide cost rates for low- and high-wage cities.

We derive these rates by combining data from multiple sources. Capital cost rates for high-wage cities were calculated by fitting a linear regression model to real-world data obtained from the B-cycle systems in 14 US cities, and from the Capital Bikeshare system in Arlington, Virginia (Arlington, 2010). Operating cost rates for high-wage cities were calculated using financial analysis data collected from the Nice Ride public bike-share program in Minnesota's Twin Cities (City of Minneapolis, 2008). Capital and operating cost rates for low-wage cities were taken from the Hangzhou (China) public bike system (Wikipedia, 2017). The above cost parameters are summarized in Table F.1.

We then calculated the daily costs per bike, per dock, and per docking station for both high- and low-wage cities. The daily cost for each item is the sum of the capital cost amortized over the item's lifecycle (assumed to be 5 years) and the operating cost. We assumed that each year had 365 days. Calculation results are also shown in Table F.1.

Table F.1. Cost rate breakdown for bike-sharing systems.

		High-wage cities	Low-wage cities
Capital cost ($/item)	Bike	1,118	57
	Dock	1,195	149
	Docking station	19,434	10,401
Operating cost ($/item/year)	Bike	719.6	148.6
	Dock	-	-
	Docking station	3,084	1,337
C_B ($/bike/day)		$\frac{(1118/5)+719.6}{365} = 2.58$	$\frac{(57/5)+148.6}{365} = 0.44$
C_D ($/dock/day)		$\frac{(1195/5)}{365} = 0.65$	$\frac{(149/5)}{365} = 0.08$
C_P ($/bike/day)		$\frac{(19434/5)+3084}{365} = 19.10$	$\frac{(10401/5)+1337}{365} = 9.36$

Bibliography

Ahuja, S., Priest, N., Vuren, T., 2003. Public transport priority schemes: Comparing microsimulation with traditional TRANSYT and LINSIG models. In: Proceedings of the European Transport Conference (ETC), Strasbourg, France.

Arlington, 2010. Notice of Award of Contract. Bicycle Share contract award for the County of Arlington, Virginia.

Beatley, T., 2014. Planning for sustainability in European cities: A review of practice in leading cities. The Sustainable Development Reader, Routledge, London.

Bicycle Dutch, 2018. New underground bicycle parking facility in Maastricht. https://bicycledutch.wordpress.com/2018/01/30/new-underground-bicycle-parking-facility-in-maastricht/ (accessed on 27 May, 2019)

Bie, Y., Liu, Z., Wang, H. 2020. Integrating Bus Priority and Presignal Method at Signalized Intersection: Algorithm Development and Evaluation. Journal of Transportation Engineering, Part A: Systems 146(6), 04020044.

Bonnette, B., 2007. The implementation of a public-use bicycle program in Philadelphia. University of Pennsylvania, Urban Studies Program.

Chang, S.K., Schonfeld, P.M., 1991. Multiple period optimization of bus transit systems. Transportation Research Part B 25(6), 453-478.

Chen, H., Gu, W., Cassidy, M.J., Daganzo, C.F., 2015. Optimal transit service atop ring-radial and grid street networks: A continuum approximation design method and compariso ns. Transportation Research Part B 81, 755-774.

Chen, P.W., Nie, Y.M., 2017a. Analysis of an idealized system of demand adaptive paired-line hybrid transit. Transportation Research Part B 102, 38-54.

Chen, P.W., Nie, Y.M., 2017b. Connecting e-hailing to mass transit platform: Analysis of relative spatial position. Transportation Research Part C 77, 444-461.

Chen, P.W., Nie, Y.M., 2018. Optimal design of demand adaptive paired-line hybrid transit: Case of radial route structure. Transportation Research Part E 110, 71-89.

Cheng, Y.H., Liu, K.C., 2012. Evaluating bicycle-transit users' perceptions of intermodal inconvenience. Transportation Research Part A 46(10), 1690-1706.

Chien, S., Schonfeld, P., 1997. Optimization of grid transit system in heterogeneous urban environment. Journal of Transportation Engineering 123(1), 28-35.

City of Minneapolis, 2008. Non-Profit Business Plan for Twin Cities Bike Share System (public version). http://www.velotraffic.com/ (accessed on April 2018).

Daganzo, C.F., 2007. Urban gridlock: macroscopic modeling and mitigation approaches. Transp. Res. B 41(1), 49-62.

Daganzo, C.F., 2010a. Structure of competitive transit networks. Transportation Research Part B 44(4), 434-446.

Daganzo, C.F., 2010b. Basic principles of system design, operations planning and real-time control. University of California, Berkeley. Course notes UCB-ITS-CN-2010-2.

Eichler, M., Daganzo, C.F., 2006. Bus lanes with intermittent priority: Strategy formulae and an evaluation. Transp. Res. B 40(9), 731-744.

Estrada, M., Roca-Riu, M., Badia, H., Robuste, F., Daganzo, C.F., 2011. Design and implementation of efficient transit networks: Procedure, case study and validity test. Transportation Research Part A 45, 935-950.

Faghih-Imani, A., Hampshire, R., Marla, L., Eluru, N., 2017. An empirical analysis of bike sharing usage and rebalancing: Evidence from Barcelona and Seville. Transportation Research Part A 97, 177-191.

Fan, W., Mei, Y., Gu, W., 2018. Optimal design of intersecting bimodal transit networks in a grid city. Transportation Research Part B 111, 203-226.

Gauthier, A., Hughes, C., Kost, C., Li, S., Linke, C., Lotshaw, S., Mason, J., Pardo, C., Rasore, C., Bradley, S., Trevino, X., 2013. The bike-share planning guide. Institute for Transportation and Development Policy, New York, NY.

Garrow, M., Machemehl, R., 1997. Development and Evaluation of Transit Signal Priority Strategies. Technical Report SWUTC/97/472840-00068-1, University of Texas at Austin.

Gleason, R., Miskimins, L., 2012. Exploring bicycle options for federal lands: Bike sharing, rentals and employee fleets. Publication FHWA-WFL/TD-12-001. FHWA, U.S. Department of Transportation.

Goodyear, S., 2014. Bixi Files for Bankruptcy, But Bike-Share Goes On. https://www.citylab.com/transportation/2014/01/bixi-files-bankruptcy-bike-share-goes/8154/ (accessed on May 2018.)

Gu, W., Amini, Z., Cassidy, M.J., 2016. Exploring alternative service schemes for busy transit corridors. Transportation Research Part B 93, 126-145.

Gu, W., Chen, H., Xuan, Y., 2015. Providing bus signal priority without damaging car discharge capacities. Conference on Advanced Systems in Public Transport, Rotterdam, the Netherlands, 19-23 July 2015.

Guler, S.I., Cassidy, M.J., 2012. Strategies for sharing bottleneck capacity among buses and cars. Transp. Res. B 46(10), 1334-1345.

Guler, S.I., Menendez, M., 2014a. Analytical formulation and empirical evaluation of pre-signals for bus priority. Transp. Res. B 64, 41-53.

Guler, S.I., Menendez, M., 2014b. Evaluation of Presignals at Oversaturated Signalized Intersections. Transp. Res. Rec. 2418, 11-19.

Gunn, A., 2018. Bicycle planning in European cities and its applicability to American cities. California Polytechnic State University, Senior project.

Gutman, D., 2017. Seattle's Pronto bike share shut down on March 31. https://www.seattletimes.com/seattle-news/transportation/seattle-pronto-bike-share-shutting-down-friday/ (accessed on May 2018.)

Hampshire, R., Marla, L., 2012. An analysis of bike sharing usage: explaining trip generation and attraction from observed demand. Transportation Research Board 91st Annual Meeting, Washington DC.

Hausman, J.A., Wise, D.A., 1978. A conditional probit model for qualitative choice: Discrete decisions recognizing interdependence and heterogeneous preferences. Econometrica 46(2), 403-426.

He, H., Guler, S.I., Menendez, M., 2016. Adaptive control algorithm to provide bus priority with a pre-signal. Transp. Res. C 64, 28-44.

Ibarra-Rojas, O.J., Delgado, F., Giesen, R., Muñoz, J.C., 2015. Planning, operation, and control of bus transport systems: A literature review. Transportation Research Part B 77, 38-75.

Kepaptsoglou, K., Karlaftis, M., 2009. Transit route network design problem. Journal of Transportation Engineering 135(8), 491-505.

Lane, K., 2015. City Council votes to expand bike share program. https://downtowndevil.com/2015/09/10/72037/city-council-votes-to-expand-bike-share-program/ (accessed on April 2018.)

Li, L., Loo, B.P.Y., 2016. Towards people-centered integrated transport: A case study of Shanghai Hongqiao Comprehensive Transport Hub. Cities 58, 50-58.

Lighthill, J., Whitham, G.B., 1955. Kinematic waves II – A theory of traffic flow on long crowded roads. Proceedings of the Royal Society-A 229, 317-345.

Lin, Y., Yang, X., Zou, N., Franz, M., 2015. Transit signal priority control at signalized intersections: a comprehensive review. Transp. letters 7(3), 168-180.

Liu, Z., Jia, X., Cheng, W., 2012. Solving the last mile problem: Ensure the success of public bicycle system in Beijing. The 8th International Conference on Traffic and Transportation Studies, Changsha, China.

Luo, J., 2011. Promising implementation of the "Mixed Waiting Zone" (translated from Chinese). Eastday.com, April 21, 2011. http://xwcb.eastday.com/c/20110421/u1a875464.html (accessed on October 2019.)

Martens, K., 2007. Promoting bike-and-ride: the Dutch experience. Transportation Research Part A 41(4), 326-338.

Ma, T., Liu, C., Erdoğan, S., 2015. Bicycle sharing and transit: Does Capital bikeshare affect metrorail ridership in Washington, D.C? Transportation Research Board 94th Annual Meeting, Washington DC.

Medina, M., Giesen, R., Muñoz, J.C., 2013. Model for the optimal location of bus stops and its application to a public transport corridor in Santiago, Chile. Transportation Research Record 2352(1), 84-93.

Midgley, P., 2009. The role of smart bike-sharing systems. In: Urban Mobility. Journeys. May. 23-31.

Midgley, P., 2011. Bicycle-sharing schemes: Enhancing sustainable mobility in urban areas. Commission on Sustainable Development. UN Department of Economic and Social Affairs, New York.

Midgley, P., 2013. The bike-share report: Hard times and hope for the future. http://thecityfix.com/blog/bike-share-report-hard-times-hope-for-future-peter-midgley/ (accessed on May 2018.)

Muñoz, B., Monzon, A., López, E., 2016. Transition to a cyclable city: Latent variables affecting bicycle commuting. Transportation Research Part A 84, 4-17.

Muthuswamy, S., McShane, W.R., Daniel, J.R., 2007. Evaluation of transit signal priority and optimal signal timing plans in transit and traffic operations. Transp. Res. Rec. 2034, 92-102.

Nadal, L., 2007. Bike sharing sweeps Paris off its feet. Sustainable transport. Institute for Transportation and Development Policy, New York, NY.

Newell, G.F., 1971. Dispatching policies for a transportation route. Transportation Science 5, 91-105.

Newell, G.F., 1993. A simplified theory of kinematic waves in highway traffic, part I: General theory; part II: Queueing at freeway bottlenecks; part III: Multi-destination flows. Transp. Res. B 27(4), 281-313.

Noland, R., Ishaque, M., 2006. Smart bicycles in an urban area: evaluation of a pilot scheme in London. Journal of Public Transportation 9(5), 71-95.

Nourbakhsh, S.M., Ouyang, Y., 2012. A structured flexible transit system for low demand areas. Transportation Research Part B 46(1), 204-216.

Nurworsoo, C., Cooper, E., Cushing, K., 2012. Integration of bicycling and walking facilities into the infrastructure of urban communities. Mineta Transportation Institute, San Jose, California.

Oke, O., Bhalla, K., Love, D.C., Siddiqui, S., 2015. Tracking global bicycle ownership patterns. Journal of Transport and Health 2(4), 490-501.

Ouyang, Y., Nourbakhsh, S.M., Cassidy, M.J., 2014. Continuum approximation approach to bus network design under spatially heterogeneous demand. Transportation Research Part B 68, 333-344.

Pucher, J., Buehler, R., 2008. Cycling for everyone: Lessons from Europe. Transportation Research Record 2074, 58-65.

Pucher, J., Buehler, R., 2012. Integration of cycling with public transportation. City Cycling, MIT Press, Cambridge, MA, 157-181.

Qiu, F., Li, W., Zhang, J., Zhang, X., Xie, Q., 2015. Exploring suitable traffic conditions for intermittent bus lanes. J. Adv. Transp. 49(3), 309-325.

Richards, P.I., 1956. Shockwaves on the Highway. Oper. Res. 4, 42-51.

Sivakumaran, K., Li, Y., Cassidy, M.J., Madanat, S.M., 2014. Access and the choice of transit technology. Transportation Research Part A 59, 204-221.

Shaheen, S., Cohen, A., Chung, M., 2009. North American car-sharing: 10-year retrospective. Transportation Research Record 2110, 35-44.

Shaheen, S., Guzman, S., Zhang, H., 2010. Bikesharing in Europe, the Americas, and Asia: Past, present, and future. Transportation Research Record 2143, 159-167.

Suzuki, M., Nakamura, H., 2017. Bike share deployment and strategies in Japan. Discussion paper for the Roundtable on Integrated and Sustainable Urban Transport, Tokyo, Japan.

Tan, C.W., Park, S., Zhou, K., Liu, H., Lau, P., Li, M., Zhang, W.B., 2006. Prediction of transit vehicle arrival times at signalized intersections for signal priority control. Intelligent Transportation Systems Conference, IEEE, 1477-1482.

Tang, Y., Pan, H., Shen, Q., 2011. Bike-sharing systems in Beijing, Shanghai, and Hangzhou and their impact on travel behavior. Transportation Research Board 90th Annual Meeting, Washington DC.

Taylor, D., Mahmassani, H., 1996. Analysis of stated preferences for intermodal bicycle-transit interfaces. Transportation Research Record 1556, 86-95.

The City of New York Government. In: http://www.nyc.gov/html/brt/html/about/buslanes.shtml (2018).

TNS Sofres, 2009. Vélib satisfactory survey. Paris: TNS Sofres.

http://velib.centraldoc.com/%20newsletter/22_bientot_2_ans_d_utilisation_votre_regard_sur_le_service (accessed on March 2018.)

Truong, L.T., Currie, G., Sarvi, M., 2017. Analytical and simulation approaches to understand combined effects of transit signal priority and road-space priority measures. Transp. Res. C 74, 275-294.

Urbanik II, T., Holder, R.W., 1977. Evaluation of Priority Techniques for High Occupancy Vehicles on Arterial Streets. Texas Transportation Institute, Texas A&M University.

Viegas, J., Lu, B., 2001. Widening the scope for bus priority with intermittent bus lanes. Transp. Plan. Techn. 24(2), 87-110.

Viegas, J., Lu, B., 2004. The intermittent bus lane signals setting within an area. Transp. Res. C 12(6), 453-469.

Wang, Z., 2013a. Towards the Modes of Managing the Urban Bike Sharing System (in Chinese). Urban Development Studies 20(9), 93-97.

Wang, H., 2013b. Public bikes in Minhang District, Shanghai (in Chinese). Eastday.com. http://sh.eastday.com/m/20130628/u1a7483831.html (accessed on March 2018.)

Watkins, K., Berrebi, S., Diffee, C., Kiriazes, B., Ederer, D., 2019. Analysis of recent public transit ridership trends.

Wen, C.H., Koppelman, F.S., 2001. The generalized nested logit model. Transportation Research Part B 35(7), 627-641.

Wieth-Knudsen, A., 2012. Bikes - A way to increase demand for public transport? Velo-city Global Conference, 194-201.

Wikipedia, 2017. Hangzhou Public Bicycle. https://en.wikipedia.org/wiki/Hangzhou_Public_Bicycle (accessed on March 2018.)

Wirasinghe, S.C., Ghoneim, N.S., 1981. Spacing of bus-stops for many-to-many travel demand. Transportation Science 15(3), 210-221.

Wu, J., Hounsell, N., 1998. Bus priority using pre-signals. Transp. Res. A 32(8), 563-583.

Xuan, Y., Daganzo, C.F., Cassidy, M.J., 2011. Increasing the capacity of signalized intersections with separate left turn phases. Transp. Res. B 45(5), 769-781.

Yang, M., Liu, X., Wang, W., Li, Z., Zhao, J., 2015. Empirical analysis of a mode shift to using public bicycles to access the suburban metro: Survey of Nanjing, China. Journal of Urban Planning and Development 142(2).

Zhou, G., Gan A., 2005. Performance of transit signal priority with queue jumper lanes. Transp. Res. Rec. 1925, 265-271.